POLITECNICO DI TORINO

MASTER's Degree in Energy and Nuclear Engineering

MASTER's Degree Thesis

Performance Analysis of Commercial and Innovative Materials aiming for Deep Biogas Cleaning

Supervisors

Prof. MASSIMO SANTARELLI

Prof. ANDREA LANZINI

PhD. MARTA GANDIGLIO

Candidate

ROBERTO PAGLINI

July 2021

Abstract

In the current challenge to contain the global warming, renewable energy sources development plays a crucial role to decarbonise the energy sector. In this context, biogas have the potential to act as a renewable energy and carbon source for energy production and chemical industry applications. Biogas production from anaerobic digestion of organic wastes sets allows this renewable energy production in the circular economy frame. Therefore, several EU projects have been and are still conducted. The Waste2Watt project [1] aims at designing flexible cleaning systems to unlock the potentialities of a biogas for CHP production through Fuel Cells. Its focuses are both on small scale applications (e.g. zootechnic effluents from farms), for which the cleaning technology is adsorption-based, and large scale applications (e.g. OFMSW use via an efficient municipal waste management), for which the cleaning technology is cryogenic separation.

The role of Politecnico di Torino, PSI Institute and ENEA Institute is to support the design of optimized absorption-based cleaning systems through commercial and innovative sorbent-materials testing. The final decision for an optimized cleaning system will merge the information about the tested materials performances, with the purchase and waste management costs in a techno-economical analysis.

Commercially available and new-on-market materials have been selected by contacting the suppliers directly, while the main biogas pollutants have been shared among the project partners, specifically, Politecnico di Torino tested H_2S and will test CH_4S.

Tests have been conducted by simulating a realistic biogas composition (CO_2, CH_4, O_2, humidity and the pollutant). A particular interest have been dedicated in analysing the sorbents both in dry, anhydrous conditions and in presence of oxygen. This interest depends on the possibility, for certain sorbents (typically impregnated activated carbons), to exploit oxygen traces to oxidize sulphur compounds within the reactor, thus improving their removal performances. Additionally, the presence of humidity can generate an internal film of liquid water in the reactor, thus adding the contribution of a liquid interface to the removal capacity.

For this reasons, sorbent materials have been analysed to evaluate the specific surface area, porosity and composition (BET analysis and XRD analysis). Test results, combined with fresh and exhausted material analysis, allow to deeply analyse the correlations between structural characteristics and macroscopic adsorption performances.

Acknowledgements

I would like to thank my tutors PhD Marta Gandiglio, Prof. Andrea Lanzini and Prof. Massimo Santarelli of the Politecnico di Torino for advising me and guiding me in this research activity. I would also like to thank Elena Rozzi, with whom I collaborated in this experimental campaign.

Roberto Paglini

Table of Contents

List of Tables VI

List of Figures VIII

Acronyms XI

1 Introduction 1

1.1 The need for a decarbonised energy mix 1

1.2 Biogas as a Controllable Energy Source 1

1.2.1 Biogas Market 2

1.2.2 Anaerobic Digestion 4

1.2.3 SOFC Technology 5

1.2.4 Former case-studies: SOFCOM and DEMOSOFC 8

1.2.5 New EU Projects: Waste2Watts 10

2 Biogas Pollutants 11

2.1 Anaerobic Digestion Gas Pollutants 11

2.2 Sulfur Compounds 11

2.3 Siloxanes 14

2.4 Other Pollutants: Halogens and Non-Methane Volatile Organic Compounds 14

3 Biogas Cleaning 15

3.1 Cleaning Technologies: an Overview 15

3.1.1 Absorption-based systems 16

3.1.2 Adsorption-based systems 18

3.1.3 Cryogenic Technology 20

3.2 Waste2Watt Project description 21

4 Materials and Methods 23

4.1 Sorbent Specifications 23

4.2 Sorbent Characterization 24
4.2.1 Results 26
4.3 Adsorption Analysis Campaign 30

5 Experimental Activity 37
5.1 Screening Tests 37
5.2 Tests with Oxygen Traces 41
5.3 Results and Comments 41
5.3.1 Future Tests Planning 48

Bibliography 50

List of Tables

1.1 Comparison of SOFC technology versus ICE technology in term of efficiency (expressed in percentage [%]). Due to the high temperature of the hydrogen combustion, no pure H_2-feeding is possible for ICEs. *ICE: 31% for the smaller size investigated, 35% for the larger one. **SOFC sees no efficiency variation with size. 8

2.1 Anaerobic Digested Gas pollutants. Papadias et al., 2012. Based on the Argonne National Laboratory database, access 15.05.2012 [24] . 12
2.2 Summary of SOFC tolerance to biogas main pollutants 13

4.1 Sorbents name, material type and suppliers, with reference to the company official web page. 23
4.2 BET Analysis result: specific surface area evaluated, evaluated at DISAT laboratory at Politecnico di Torino in march 2021. Results compared to those from ENEA analysis on the same materials and literature reference to tests on same/similar materials. 28
4.3 L/D ratio is set to the minimum value of 3 to avoid the formation of preferential pathways. GHSV is set to 1500 as standard working parameter able to guarantee a sufficient residence time for the mass transfer to occur. 30
4.4 Reactor geometry data 33

5.1 Gas composition used for screening tests. Under the 'preliminary' column are reported the gas composition data used for dry screening in absence of oxygen, to assess the baseline performances of the sorbents. The column 'O_2, RH contains the data on gas composition for more realistic tests, in presence of oxygen and humidity. 38
5.2 Tests with Oxygen traces (0.5% O_2) 41
5.3 Screening test results in term of breakthrough time and adsorption capacity 42

5.4 Envirocarb STIX replicas results comparison. Relative error refers to the first STIX test. 44
5.5 Sorbent materials to be tested and notes on their main characteristics 48
5.6 Regeneration process suggested by the respective suppliers 49

List of Figures

1.1 Evolution of biomethane production in Europe (EU plus non EU European countries) between 2011 and 2019 (ktoe) [5]. 3

1.2 Number of biogas producing plants in Europe in 2019 [5]. Different scales for Germany, Italy and UK. 3

1.3 Schematic representation of biogas generation via anaerobic digestion [8] 6

1.4 DEMOSOFC plant layout. The higher block represents the digester, the gas holder and the chiller, a component needed according to many sorbents producing companies. The lower block represents the two-stage cleaning unit for sulphur and siloxanes [22] 9

3.1 Plant layout of an absorption-based system with a cleaning column (scrubber), a regeneration column, and a flash column for the recovery of absorbed methane. [32] 17

3.2 Sitthikhankaew et al., in 2014 analysed the effect of oxygen and humidity on KOH-impregnated activated carbons, their results shown a significant increase in activated carbons performance towards H2S adsorption, due to the deposition of elemental sulfur or the formation of sulfuric acid in the water film originated by humidity in the material's pores [43] 20

3.3 Schematic representation of a cryogenic separation system for LBM production [44] 21

4.1 Schematic of the BET Analyzer lines in desorption mode, ASAP 2020 PLUS window. 24

4.2 Sample Tube heated in desorption mode. The sample is heated through an electric heater and covered in an insulation coating. . . 25

4.3 Sample Tube submerged in a liquid nitrogen bath, testing mode . . 26

4.4 Adsorption-Desorption curves: BET Analysis from Politecnico di Torino. Adsorption Capacity for N_2 is expressed as standard volume per unit of mass. 29

4.5 Correlation between L/D ratio and Adsorption Capacity [45] 31
4.6 P&I diagram of the test station. It is possible to distinguish MFCs, the bubbler and the detectors for humidity and for hydrogen sulfide 32
4.7 Test station gas lines. Each line is fed through a MFC and contains one specific flow. As shown by the arrows, each line is bifurcated. Following the main direction of the pipes (yellow arrow), the flows are merged and sent to the bubbler for humidification (blue circle), the alternative pathway (brown arrow) merges the flow and bypasses the bubbler (red circle). 33
4.8 Reactor without coating 34
4.9 Top side of the test station: the reactor and humidity sensor are shown on the right 35
4.10 H_2S Detector 36

5.1 Display of the FlexLogger measurement in real time (red line on graph). The three windows on the top right corner are the user interface to the MFC communication systems through which it is possible to define the flowrate of each gas. 40
5.2 Graphical representation of the adsorption capacity of the sorbents at breakthrough (from Table 5.3) 43
5.3 Envirocarb ACs, STIX repetitions and AP4-60, adsorption profile . 44
5.4 SulfaTrap R7HB adsorption profile 45
5.5 Norit RGM3 replicas adsorption profile 46
5.6 BioClean Gas Granular adsorption curve 47

Acronyms

HTFC

High Temperature Fuel Cell

OFMSW

Organic Fraction of Municipal Solid Wastes

GHG

Greenhouse Gases

SOFC

Solid Oxide Fuel Cell

WWTP

Wastewater Treatment Plant

DMS

Dimethyl Sulfide

ICE

Internal Combustion Engine

PM

Particulate Matter

VOC

Volatile Organic Compound

AD

Anaerobic Digestion

YSZ
Yttria Stabilized Zirconia

toe
tonnes of oil equivalent

SDS
Sustainable Development Scenario

AC
Activated Carbon

PAC
Powder Activated Carbon

GAC
Granular Activated Carbon

NG
Natural Gas

GHSV
Gas Hour Space Velocity

LBM
Liquefied Biomethane

RH
Relative Humidity

BT
Breakthrough Time

EBA
European Biogas Association

HTGT
High Temperature Gas Turbine

MFC

Mass Flow Controller

Chapter 1

Introduction

1.1 The need for a decarbonised energy mix

In order to mitigate the phenomenon of Climate Change, it is mandatory to reduce anthropogenic emissions of green house gasses. As the energy sector is the main contributor to GHG emissions, it is mandatory to increase the share of carbon neutral and carbon free energy sources in the global energy mix.
Current European policies aim to reach the current goal of containing the mean global temperature increase below 1.5 °C, and to achieve climate-neutrality by 2050 [2].
Along with the other non-carbon emitting energy sources, as nuclear, solar photovoltaic and wind power, biogas produced by the anaerobic digestion of organic wastes can play an important role to recover energy from a renewable source whilst disposing of a waste, which can eventually be converted into a fertilizer or soil conditioner, merging both the renewable energy sources and the circular economy frameworks.

1.2 Biogas as a Controllable Energy Source

Biogas is a mixture of methane and carbon dioxide generated from biomass which undergoes an anaerobic digestion process. Bacteria exploit carbohydrates, proteins and fatty acids to sustain their metabolic needs, thus converting them into organic acids, acetate and, finally, a methane and carbon dioxide that, being gasses, can be recovered from the top of the digester as a mixture named "biogas".
Being a methane-containing gas mix, biogas can be exploited for several energy applications, allowing this energy source to combine one major positive aspect of fossil fuels which cannot be associated to conventional RES: the reliability in terms

of lack of intermittency.
As a renewable energy source, its emissions are carbon neutral, and it is generated by anaerobic digestion of biomass, therefore its production can be coupled with those processes which produce biomass waste, such as sludge in wastewater treatment plants (WWTPs), manure and slurry in farms, or the organic fraction of municipal solid waste from separate collection systems (OFMSW).
Being biomass-based, biogas is a renewable energy source with carbon neutral emissions which can be used for combined heat and power production (CHP) on the end-user side of the electricity and natural gas grids, leading to a lower energy demand of said plants whilst treating its waste. Once the digestion is completed, the remaining waste, known as digestate, can be post-treated for agricultural valorization purposes, as fertilizer, or thermochemically transformed for further energy or chemical by-products recovery [3].

Biogas Uses

Biogas can be exploited for several application: from direct heat production to CHP production, and even to its upgrade to biomethane and its injection into the NG grid.
Direct biogas combustion for heat production is a relatively low cost application, suitable for small size plants. Conversely, more refined applications like biomethane grid injection and biogas-fed ICEs and HTGS are more costly, therefore suitable for large plants in which the unit cost is reduced by size-effect.

1.2.1 Biogas Market

Biogas is expanding worldwide in the recent years, with Europe as largest producer in 2018 [4]. The worldwide production has been estimated to be approximately 35 Mtoe, with a worldwide potentiality of 570 Mtoe.
The biogas market across Europe has expanded significantly in the last decade (Figure 1.1). According to the European Biogas Association (EBA), this can be related to the increasing share of biogas and biomethane related technologies, such as transport decarbonization through biomethane use as vehicle fuel and liquid biomethane use as maritime and railway fuel [5].

Since biogas is the basis for biomethane production, its production across Europe has also increased significantly. In 2019, the year of the study, Germany, Italy and UK were the top three European countries for number of biogas producing plants, as shown in Figure 1.2.

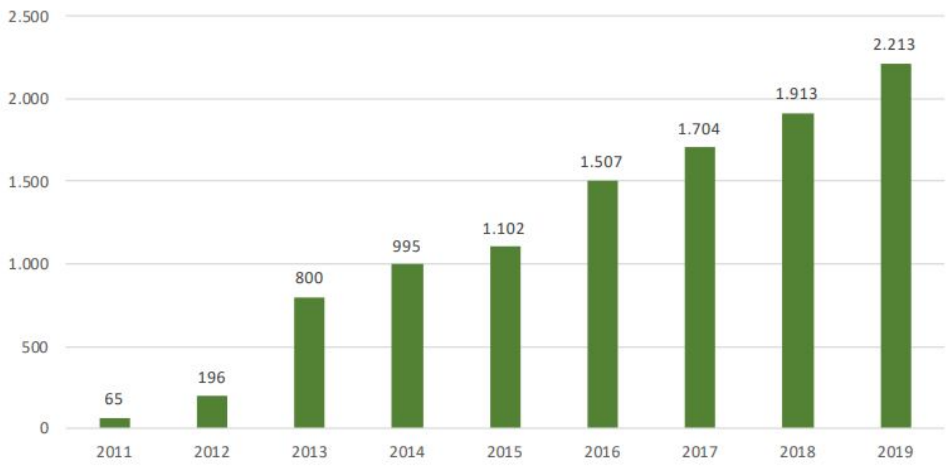

*EU27 + UK + Switzerland + Norway + Iceland

Source: *European Biogas Association, EBA*

Figure 1.1: Evolution of biomethane production in Europe (EU plus non EU European countries) between 2011 and 2019 (ktoe) [5].

Moreover, the article points out that sustainable policies also aim at avoiding conflict between energy production and agricultural resources. For this reason first generation biomass, as energy crops, Germany main biogas source in 2019, is expected to progressively be replaced by second generation biomass, as agricultural residues, and other bio-wastes, as OFMSW and sewage sludge.

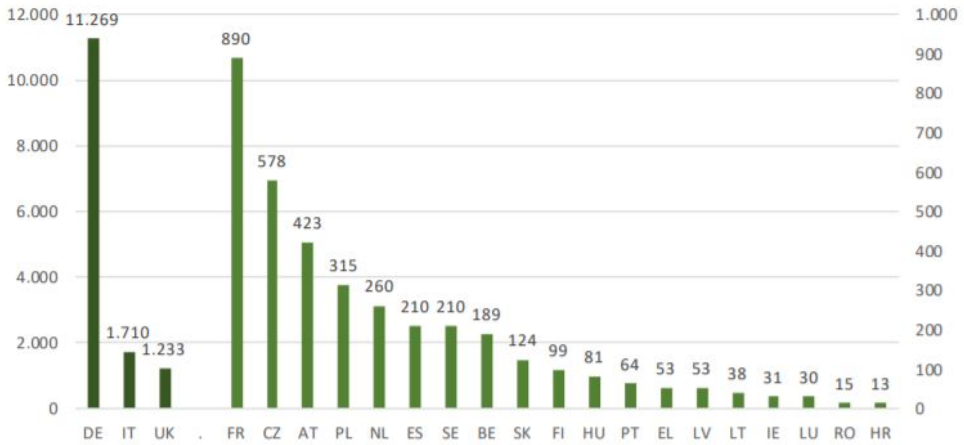

Figure 1.2: Number of biogas producing plants in Europe in 2019 [5]. Different scales for Germany, Italy and UK.

IEA's Sustainable Development Scenario (SDS) suggests that, in order to achieve the climate goal of containing the global mean temperature increase "well below 2°C", biogas is expected to "grow by 40% over the period to 2040" with large opportunities in Pacific Asia, as an alternative to natural gas, whose demand is growing rapidly [4]. This growth can be associated with a better exploitation of biomass feedstocks, mainly bio-wastes in the framework of circular economy. Additionally, biogas and biomethane use as cooking gas would grant several environmental and health-related benefits to those communities where the main cooking fuel is conventional biomass, which is characterized by a strongly inefficient combustion if compared to other fuels, thus leading to household air pollution and its consequential impact on human health [6].

1.2.2 Anaerobic Digestion

The set of biological processes contributing to biogas generation is named anaerobic digestion (AD).
AD occurs when biological material is confined in an anaerobic environment, to allow bacterial activity to consume carbohydrates, fatty acids and proteins to sustain their metabolic activity. The main of metabolic reactions are:

1. Hydrolysis: complex organic molecules are hydrolysed into their monomers.

$$OH-[1]-[2]-[3]-[4]-H+H_2O \rightarrow OH-[1]-[2]-H+OH-[3]-[4]-H \tag{1.1}$$

2. Acidogenesis: in this phase, carbohydrates, fatty acids and protein monomers are converted into organic acids, alcohols, hydrogen and carbon dioxide through fermentation.

3. Acetogenesis: in this phase, organic acids and alcohols are converted into acetic acid.

$$CH_3CH_2COOH + 2H_2O \rightarrow CH_3COOH + 2H_2 \tag{1.2}$$

4. Methanogenesis: in this last phase, acetic acid is converted into methane and carbon dioxide. Additionally, elemental hydrogen generated in previous reactions converted into methane using CO_2. Hydrogen-consuming bacteria and hydrogen-generating ones act in synergy [7].

$$CH_3COOH \rightarrow CH_4 + CO_2 \tag{1.3}$$

$$4H_2 + CO_2 \rightarrow CH_4 + 2H_2O \tag{1.4}$$

A schematic representation of this set of reactions in provided in Figure 1.3. Other byproducts are generated along methane and carbon dioxide, for example, sulfur compounds originate other sulfur-based pollutants. The most common S-based pollutant is hydrogen sulfide (H_2S), followed by organic ones, named thiols/mercaptans. Additionally, the biomass origin cause other pollutants to enter the biogas stream, sludge from WWTPs is richer in siloxanes (silicon compounds) because they are widely used in the cosmetic industry, therefore are collected in the sewage water and its sludge.

In Chapter 2 there is a more detailed description of the main biogas pollutants, in terms of nature, origin, and potential detrimental effects on SOFCs.

It is worth to notice that not the entirety of the organic material can be converted into methane and carbon dioxide. Leftover organic matter takes the name of digestate, and can be potentially exploited as soil conditioner for agricultural application, thus entering the economic balance of the plant.

Biogas producing plants perform anaerobic digestion in a designed structure, defined 'Digester', where fresh biomass can be continuously supplied and biogas can be collected from the top of the digester.

As bacteria operating anaerobic digestion work in mesophilic condition (35 - 40 °C), the digester must be continuously heated to sustain its temperature. Plants that directly consume biogas for CHP applications can use part of the SOFC generated heat for this purpose.

1.2.3 SOFC Technology

Biogas utilization for electricity production can be achieved in different ways. The most obvious one would be its combustion with oxygen in an internal combustion engine (ICE), but this solution requires the initial conversion of biogas energy into heat, so its later conversion into mechanical work has an upper bound, Carnot's efficiency, associated to the temperature level at which heat becomes available for the engine cycle.

To bypass this limit, it is possible to exploit coupled electrochemical reactions (oxidation-reduction) to achieve a direct biogas utilization for electricity production. Among the different types of fuel cell on the market, those working at high temperature (HTFC) are the only ones able to process a carbon-containing fuel. Low temperature fuel cells would be damaged by solid carbon deposition at the catalytic sites and would clog the pores, causing the cell irreversible detriment. Therefore, low temperature fuel cells require to be fed by hydrogen at high purity standards.

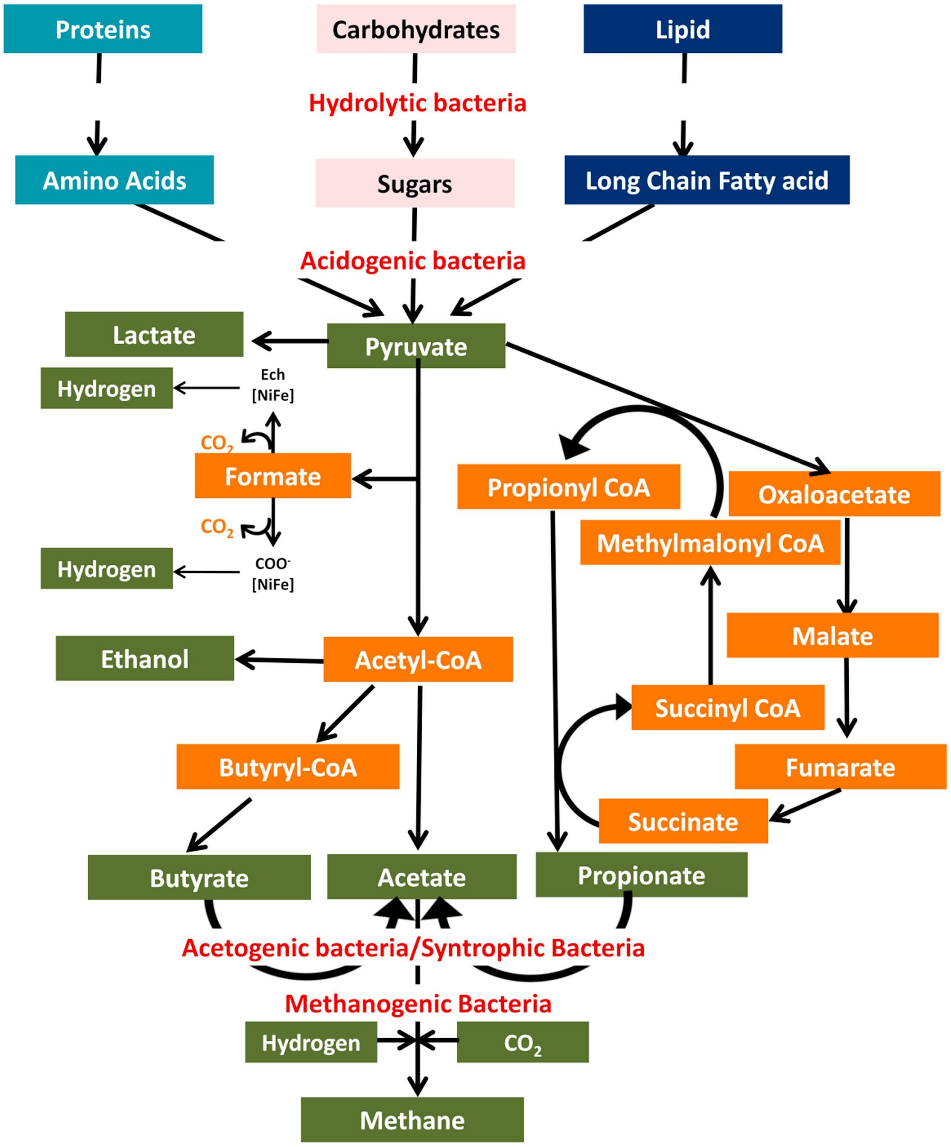

Figure 1.3: Schematic representation of biogas generation via anaerobic digestion [8]

Conversely, Solid Oxide Fuel Cells (SOFC) are a subcategory of High Temperature Fuel Cells working around 800 °C, thus able to process biogas without the need for its thermochemical conversion into hydrogen. Their ceramic electrolyte (mainly YSZ = Yttria-Stabilized-Zirconia, and ceria) allows oxygen ions to flow from the cathode to the anode, where it can react with the fuel. The electrochemical reaction at the cathode is:

$$2O_2 + 8e^- \rightarrow 4O^{2-} \tag{1.5}$$

The electrochemical reaction at the anode is:

$$CH4 + 4O^{2-} \rightarrow CO_2 + 2H_2O + 8e^- \tag{1.6}$$

Although methane can be directly oxidized at the three-phase boundaries, due to the production of water, to the high temperature of the system, and the presence of the catalyst, methane is locally converted to carbon monoxide and hydrogen, which are the actual charge exchangers of the anode:

$$CH_4 + H_2O \rightarrow 3H_2 + CO \tag{1.7}$$

Carbon dioxide, present in the biogas and originated locally from CO oxidation, can also take active part in the system according to the dry methane reforming:

$$CH_4 + CO_2 \rightarrow H_2 + 2CO \tag{1.8}$$

Additionally, hydrogen is also produced by water gas shift from CO and H_2O:

$$CO + H_2O \rightarrow H_2 + CO_2 \tag{1.9}$$

Comparison between SOFC and ICE

SOFC technology advantages lies in both electrical efficiency and lack of pollutants. As stated previously, efficiency is enhanced by the fact that the fuel is electrochemically oxidized in a set of reactions that provides both voltage difference and an electron flow to generate electric power. The resulting improvement in efficiency is shown in Table 1.1.

The lack of combustion coupled with the high purity of the fuel for SOFC applications cause SOFC to have an extremely clean anode exhaust:

- NO_X emissions are limited due to the use of the fuel, which does not contain prompt and fuel NO_X, and due to the fact that oxidation occurs through oxygen-ion electrochemical reactions with the fuel, avoiding air nitrogen to oxidize into thermal NO_X.
- SO_X emissions are limited by the low amount of sulfur in SOFC fuel, caused by the stringent SOFC requirements to avoid catalyst poisoning (2 ppm_v is the limit for H_2S [16]).
- Particulate Matter emissions are limited by the gaseous nature of the fuel.

ICE	SOFC	fuel notes	ref.
43.7	49.8	biogas + 10% H_2	[9, 10]
44.3	49.4	biogas + 10% H_2	[9, 10]
39.0 - 44.9	49.7-49.9	biogas	[9, 10, 11, 12, 13]
36.9-46.6	50.8	pure CH_4	[9, 10, 12, 11]
-	45.5	pure H_2	[9, 10]
31 - 35*	51.1**	partially upgraded for SOFC	[14]
38.0	53.0	biogas specific composition for a real plant	[15]

Table 1.1: Comparison of SOFC technology versus ICE technology in term of efficiency (expressed in percentage [%]). Due to the high temperature of the hydrogen combustion, no pure H_2-feeding is possible for ICEs.
*ICE: 31% for the smaller size investigated, 35% for the larger one.
**SOFC sees no efficiency variation with size.

- Volatile Organic Compounds emissions are removed in the cleaning unit as well. This step is needed as VOCs have a detrimental effect on the removal of other biogas contaminants.
- CO emissions are limited due to its low amount in biogas. Additionally, its presence can be further limited due its consumption in dry-reforming reactions at the anode catalyst [17].

The last main advantage SOFC technology lies in its modularity, therefore the efficiency is independent from the system size. Conversely, ICE efficiency is strongly affected by the plant size.

1.2.4 Former case-studies: SOFCOM and DEMOSOFC

SOFCOM is a European project started in 2011 whose aim was the demonstration of technical feasibility and efficiency of CHP production through SOFC technology, fed by biogas and biosyngas, coupled with a CO2 recovery system [18, 19]. This plant shows the full potential of the circular economy parading being a quadrigeneration plant which produces heat and power for internal consumption, demineralized water from the CO2 separation unit, and micro-algae potentially available for other applications.
DEMOSOFC is a European project started in 2015 whose aim is to demonstrate the techno-economic feasibility of the first high-efficiency CHP plant using medium size Solid Oxide Fuel Cells (SOFCs) [20, 21]. The SOFC system is installed in the WWTP of Collegno, Turin (IT), and exploits the biogas produced locally by sludge

anaerobic digestion, providing 174 KW of electricity, entirely used for the plant internal consumption, and 90 KW of recovered thermal energy for the digester heating needs.

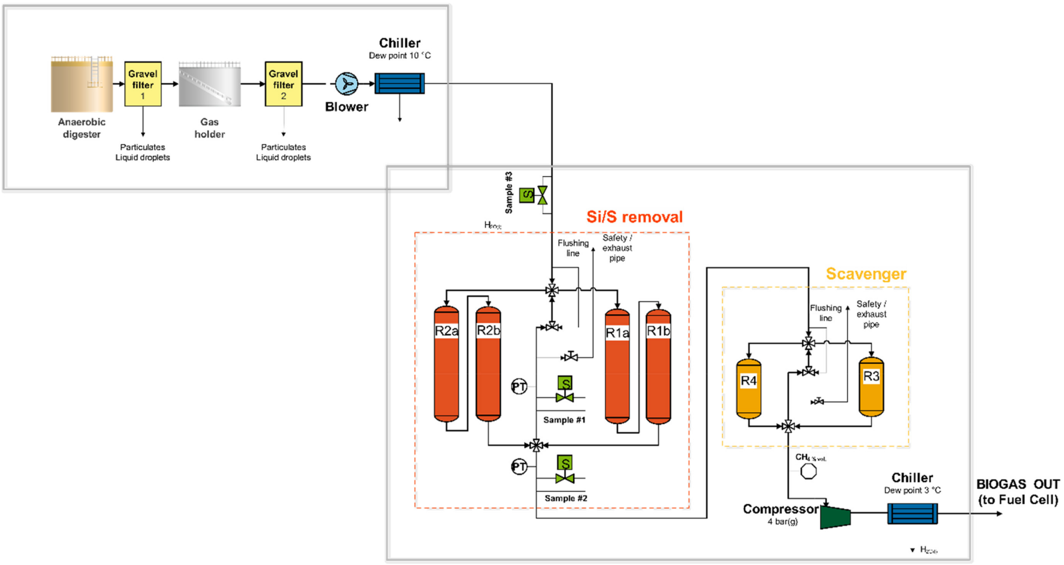

Figure 1.4: DEMOSOFC plant layout. The higher block represents the digester, the gas holder and the chiller, a component needed according to many sorbents producing companies. The lower block represents the two-stage cleaning unit for sulphur and siloxanes [22]

The DEMOSOFC plant is shown in Figure 1.4. The raw biogas recovered from the Anaerobic digester is filtered for liquid droplets removal before being stored in the gas holder, which acts as storage to couple production and use. Before use in the SOFC system, a two-stage cleaning system removes sulphur compounds and siloxanes, which have a detrimental effect on the SOFC stacks (as reported in Chapter 2). Since adsorption beds lose their cleaning performance if water vapour condensation causes pore-clogging. Therefore, a chiller is placed between the second particle filter and the first adsorption bed.

As shown in the figure, each stage has two identical beds, so that once once bed reaches the breakthrough (i.e., the pollutant outlet concentration reaches a non-zero target value which sets the beginning of the exponential growth profile) the other one can be used to continue normal operation whilst the material in the first bed is changed with fresh one.

1.2.5 New EU Projects: Waste2Watts

Waste2Watts follows the steps of previous projects, aiming at a developing flexible cleaning systems for Fuel Cell-based CHP production from different biogas sources: OFMSW, agricultural wastes, zootechnical effluents and industrial bio-wastes [1]. The main distinction sets in the project concerns the plant scale: small scale ones work on biogas generated from farms biowastes, and the cleaning technology is adsorption-based. Conversely, large industrial sites biowaste, along with OFMSW, is exploited in large scale plants. In this scenario, cleaning is performed through a cryogenic system developed by Biokomp company[23].
The details concerning the development of this study in the Waste2Watts framework will be described in section 3.2.

Chapter 2

Biogas Pollutants

2.1 Overview of Anaerobic Digestion Gas Pollutants

The proper employment of biogas as an energy source requires to match strict cleaning requirements, as different pollutants originally present in the biomass (or generated along with biogas during AD) enter the stream of biogas and become hazardous to human's health, to the environment, and to the device used for power generation, as some pollutants have a detrimental effect on ICEs and HTFCs.
This chapter focuses on biogas main pollutants, their origin, their impact on people, on the environment, and on fuel cells. Table 2.1 contains a detailed classification of biogas pollutants, based on the Argonne National Laboratory data [24], while Table 2.2 contains a summary of SOFC tolerance to biogas main pollutants (H_2S, siloxanes and halogens).
It is worth noticing that not all biogas pollutants have a direct detrimental effect, but their presence in the cleaning unit can affect the system performance and limit its removal efficiency, thus exposing the SOFC stack to detriment.

2.2 Sulfur Compounds

Sulfur compounds represent a treat to both machines, human, and environmental health. Their corrosive nature has a detrimental effect on the internal surfaces of the pipes, sulfur oxidation leads to sulfur oxides generation, which are irritating to

Class	Chemical Name	Formula	Max [ppm]	Average [ppm]
Siloxanes	(D4) Octamethylcyclotetrasiloxane	C8H24O4Si4	20.144	0.825
Siloxanes	(D5) Decamethylcyclopentasiloxane	C10H30O5Si5	18.129	1.689
Siloxanes	(L2) Hexamethyldisiloxane	C6H18OSi2	2.26	0.115
Siloxanes	(L3) Octamethyltrisiloxane	C8H24O2Si3	0.465	0.061
Sulfur Compound	Hydrogen sulfide	H2S	2897	400
Sulfur Compound	Methanethiol (Methyl mercaptan)	CH4S	1.07	0.08
Sulfur Compound	Carbon disulfide	CS2	0.05	0.05
Sulfur Compound	Dimethyl sulfide (DMS)	C2H6S	0.04	0.04
Halocarbons	Methylene chloride (Dichloromethane)	CH2Cl2	0.052	0.052
Halocarbons	Chloroform (Trichloromethane)	CHCl3	0.009	excl.
Halocarbons	Carbon tetrachloride	CCl4	0.005	excl.
Halocarbons	Chloroethene (Vinyl chloride)	C2H3Cl	0.119	0.119
Halocarbons	1,2-Dichloroethane	C2H4Cl2	0.308	0.157
Halocarbons	Trichloroethylene	C2HCl3	excl.	excl.
Halocarbons	1,1,2-Trichloroethane	C2H3Cl3	N.A.	N.A.
Halocarbons	Tetrachloroethylene	C2Cl4	0.1	0.1
Halocarbons	Chlorobenzene	C6H5Cl	0.693	0.255
Halocarbons	Dichlorobenzene (all isomers)	C6H4Cl2	0.61	0.254
Halocarbons	Trichlorofluoromethane (R-11)	CCl3F	0.004	0.004
Halocarbons	Chlorodifluoromethane (R-22)	CHClF2	N.A.	N.A.
Alkanes	Ethane	C2H6	51	40
Alkanes	Propane	C3H8	2	1
Alkanes	Butane	C4H10	1.3	0.7
Alkanes	Pentane	C5H12	15	7
Alkanes	Hexane	C6H14	108	25.144
Alkanes	Heptane	C7H16	0.358	0.358
Alkanes	Octane	C8H18	0.275	0.221
Alkanes	Nonane	C9H20	6.2	1.246
Aromatic	Benzane	C6H6	0.85	0.168
Aromatic	Toluene (Methylbenzane)	C7H8	2.274	1.037
Aromatic	Ethylbenzene	C8H10	5.911	1.251
Aromatic	Xylenes (o-, m-, p-, mixtures)	C8H10	4.095	0.784
Aromatic	1,3,5-Trimethylbenzene	C9H12	1.859	1.859
Aromatic	1-Methyl-4-propylbenzene (p-cymene)	C10H14	3.072	1.157
Cyclic	Cyclohexane	C6H12	excl.	excl.
Cyclic	Methylcyclohexane	C7H14	0.13	0.13
Cyclic	Dimethylcyclohexane (all isomers)	C8H16	0.39	0.39
Cyclic	Limonene	C10H16	48.9	9.729
Alcohol	Ethanol	C2H6O	N.A.	N.A.
Alcohol	2-Propanol (Isopropyl alcohol)	C3H8O	N.A.	N.A.
Ester	Ethyl acetate	C4H8O2	N.A.	N.A.
Ester	Ethyl butanoate (Butanoic acid)	C6H12O2	N.A.	N.A.
Ether	Dimethyl ether	C2H6O	N.A.	N.A.
Ether	2-methoxy-2-methyl-propane (MTBE)	C5H12O	N.A.	N.A.
Ether	Acetone	C3H6O	N.A.	N.A.
Ketone	2-Butanone (Methyl ethyl ketone)	C4H8O	N.A.	N.A.
Ketone	4-Methyl-2-pentanone (MIBK)	C6H12O	N.A.	N.A.

Table 2.1: Anaerobic Digested Gas pollutants. Papadias et al., 2012. Based on the Argonne National Laboratory database, access 15.05.2012 [24]

Pollutant	tolerance	unit	ref.
H_2S	<1	ppm(v)	[16, 25]
Siloxanes	<100 to <10	ppb(v)	[16, 25]
Halogens	<5	ppm(v)	[25]

Table 2.2: Summary of SOFC tolerance to biogas main pollutants

human's breathing system and precursors of acid rains, leading to severe damages to the environmental and to structures. This is mainly true for internal combustion engines, however, when using biogas to feed HTFCs, sulfur can convert the metal oxide used as catalyst to a metal sulfide, inactivating it.
The main sulfur-based pollutant in biogas is hydrogen sulfide, although sulfur organic compounds as mercaptane (CH_4S) and dimethyl sulfide (DMS) can also have a significant effect.

Hydrogen Sulfide

Hydrogen sulfide is a toxic and flammable gas. As an inorganic sulfur compound, it sets a treat for both human health and for environment quality. Its presence in raw biogas can be related to dimethyl sulfide and methyl mercaptane degradation due to methanogenic bacteria population [26].
It is a corrosive gas, therefore its presence in the biogas stream must be contained, and its concentration must be significantly lowered before any application of the gas, whether it is its combustion in internal combustion engines, its upgrade to biomethane, its shift to bio-syngas or, as it is the case for this project, its electrochemical oxidation in SOFC. Electrochemical systems are more sensitive towards sulfur than thermochemical ones, as sulfur converts the metal oxide catalyst into a metal sulfide, which has no catalytic effects. The result is the irreversible degradation of the cell performances [27].

Organic Sulfur Compounds

Organic sulfur can be found in raw biogas due to the presence of methionine in the biomass feed, whose digestion generate methyl mercaptan (CH4S), which can be methylated to generate dimethyl sulfide (DMS) [26].
As well as hydrogen sulfide, organic sulfur compounds have corrosive effects on metal pipes and detrimental effect on SOFC catalysts too, but their effect and poisoning dynamic have not been investigated in detail as the one of H_2S.

2.3 Siloxanes

Siloxanes are linear or cyclical molecules characterized by silicon, often exploited in cosmetic production. Therefore, their presence is particularly abundant in WWTP sludge and, due to their volatility, they enter the raw biogas stream from the digester [24].

Siloxanes' effect is the deposition of solid silica on internal surfaces and SOFC catalyst poisoning [16, 28].

2.4 Halogens and Non-Methane Volatile Organic Compounds

Among the halogenated compounds, those found as biogas pollutants are mainly chlorine-containing (HCl), and secondly fluorine and bromine-containing species (HF).

In term of detrimental effects on SOFC, chlorine compounds are able to react with nickel-based catalysts converting it into $NiCl_2$ [29], which can sublimate from the catalyst surface and precipitate on the cermet anode, causing microstructural damages.

Anaerobic digestate gas chlorine content can be low enough to match SOFC tolerances, allowing the clean-up section design to not focus on halogen pretreatment [30].

Non-methane volatile organic compounds are hydrocarbons, alcohols, alkane and aromatic compounds usually found in low concentrations such that no significant poisoning effect can take place, but they can negatively affect adsorption-based siloxane removal [24].

Chapter 3

Biogas Cleaning

3.1 Cleaning Technologies: an Overview

Biogas applications require to match specific quality criteria. Therefore, different types of cleaning technologies can be implemented to optimize decontamination costs.

Biogas more analysed contaminant is H_2S, whose content can be considerably lowered already in the digester using iron salts. As shown in Equation 3.1, iron chlorine precipitates sulfur on the bottom of the digester. This technology allows to obtain a biogas flow with up to 50 ppm(v), as below this value it is economically unfeasible.

As iron salts are already used in WWTPs to precipitate phosphorus, which would cause water eutrophication causing its biogas to have a relatively limited amount of H_2S (below 100 ppm(v)) [31].

$$2FeCl_3 + 2H_2S \rightarrow 2FeS + S + 6HCl \tag{3.1}$$

Although certain contaminants can be reduced in content directly by adding iron salts in the digester, it is necessary to implement a designated cleaning system to downstream-technologies tolerance criteria. Cleaning can be achieved by exploiting three main physi-chemical phenomena: absorption, adsorption and phase separation. The choice depends on the tolerance of the user and the techno-economic analysis of the system.

Absorption is a volumetric effect: gas dissolution in a liquid through scrubbing, and it is based on Henry's Law, adsorption is a surface effect where gas molecules are bound to the solid surface through intermolecular forces. Finally, phase separation can be achieved through a relatively young technique which is cryogenic separation,

a concept in where the different condensation temperatures of the pollutants are exploited to liquefy them and separate them from the clean biogas stream through gravity.
In this chapter, an overview over biogas cleaning and upgrading technology will be presented according to the following order:

- Absorption-based Systems
  - Water Scrubbing
  - Organic Solvents and Chemical Scrubbing
- Adsorption-based Systems
  - Activated Carbons
  - Metal Oxides and Hydroxides
  - Zeolites
- Cryogenic Separation

3.1.1 Absorption-based systems

Absorption technologies working principle is the different solubility of gaseous compounds in specific solvents, which are used to scrub the gas flow to modify its composition and obtain higher methane content. These technologies are almost exclusively implemented for biogas upgrading, exploiting the difference in solubility of carbon dioxide in water, or other solvents, compared to methane (26 times higher in water, working at 6 to 10 bar and 40 °C [32, 33]).
A simplified scheme of an absorption-based plant is provided in Figure 3.1. This layout refers specifically to a water scrubbing plant, but the main characteristics can be generalised for organic solvents and chemical scrubbing as well. The main difference may lie in the fact that the latter technologies are more selective, therefore it may not be necessary to use flash column to limit CH_4 losses. Additionally, in the specific case of water scrubbing in a WWTP, which provides clean water as main industrial activity, it could become economically feasible to avoid regeneration and to continuously consume fresh water provided by the plant.

Water Scrubbing

Water scrubbing works with pressurized and pre-treated gas. It allows to reach methane purity standards for grid injection (80% to 99%, according to the non-condensable gas content [34]).

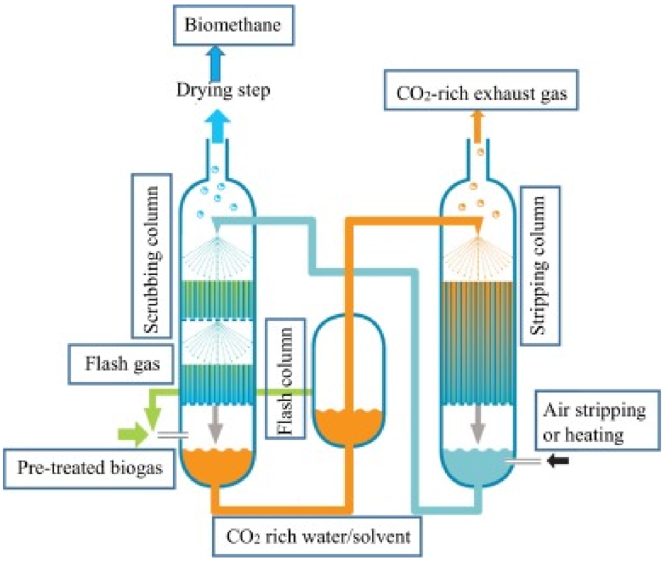

Figure 3.1: Plant layout of an absorption-based system with a cleaning column (scrubber), a regeneration column, and a flash column for the recovery of absorbed methane. [32]

The main criticalities of water scrubbing are the high water consumption, which requires water regeneration unless the plant is located in a WWTP, where clean water is locally generated and made available for the scrubber [33, 35, 36].
Water regeneration requires a heat supply combined with air stripping, which sets another limit to H_2S removal, which can reduce elemental oxygen to water, causing the deposition of elemental sulfur [35]. In this case it is needed to use an inert gas for regeneration.

Organic Solvents and Chemical Scrubbing

Organic solvents, as dimethyl ether and methanol, can be used for biogas scrubbing oriented towards its upgrading to biomethane, and theoretically, to co-remove hydrogen sulfide along with carbon dioxide [33].
As for water scrubbing, the working principle exploited with organic solvents is physisorption. CO_2 solubility is considerably higher, thus enhancing the performance of removal.
The main downside of this technology is the related to the difficulty in the regeneration process, which is a direct consequence of the higher solubility of CO_2 and H_2S. As previously stated, organic solvents are able to remove hydrogen sulfide, but its high solubility further increases the difficulties in the regeneration process,

requiring a higher desorption temperature and cooling duty [33]. As a consequence, hydrogen sulfide is often removed among other pollutants in the pre-treatment process. Therefore, organic solvents are used exclusively as an upgrading technology, able to reach 98% methane purity [33, 37].

Chemical scrubbing employs amine-based solutions to target acid gasses (CO_2 and H_2S), allowing its use for simultaneous partial cleaning while upgrading.

The methane content of the upgraded stream can reach 99%, while the methane content of the exhaust gas, used for regeneration is significantly low, and can be sent to disposal (vented) without the need for a flaring system [32].

Considerations on Absorption-based Technologies

All absorption-based technologies proved to be interesting for biogas upgrading goals only. Due to the need for a pre-treatment systems to remove those contaminants under our analysis, and due to the inevitable loss of carbon dioxide, that would preclude a proper exploitation of dry reforming in the SOFC, all absorption-based systems showed no interesting application in the Waste2Watts project framework.

3.1.2 Adsorption-based systems

Adsorption-based systems work according to inter-molecular interactions which bound pollutants on the active surface of a solid matrix, often in granular form or as powder. Due to the working principle of this phenomenon, the key factor is the specific surface area, the surface in contact with the gas flow per unit of mass.

Typical materials are activated carbons, metal oxides, and zeolites.

As for absorption technologies, adsorption ones can also be enhanced through chemical interactions at the active sites which locally convert the pollutants to be removed in other species, which are easier to fix on the solid surface.

Activated Carbons

Activated carbons are typical adsorbent materials, often exploited for a wide range of filtering-related applications.

Activated carbons are carbon-based solids originated from coal or biomass, which underwent an activation process to increase the number of micropores and active sites via an acid or basic bath, or though a blast of high temperature gasses [38, 39]. The latter alternative allows to exploit gassification chars as activated carbons, thus improving the economical balance of a gassification plant.

Adsorption-based systems often exploits activated carbons as powder or granular pellet (PAC, GAC) [40].

The activation process can also be enhanced through an impregnation process, which increases the metal content on the surface, and its active sites, to improve an adsorbent performance.

Metal Oxides

Metal oxides have good performances when removing hydrogen sulfide and siloxanes. When dealing with sulfur components, the working principle is the conversion of the metal oxide into a metal sulfide. This process is potentially reversible, via oxidation, although solid sulfur deposition may take place as well, having a detrimental effect on the sorbent and limiting is useful life in term of number of regenerations.

Zeolites

Zeolites have been subject of research for various applications, from water purification to catalytic cracking. In the energy sector, zeolites are already exploited for the removal of carbon dioxide and elemental nitrogen from natural gas to obtain a less acid gas with a higher energy content [41], and for carbon capture and sequestration from exhaust gasses [42].

Zeolites' background in the energy sector makes them suitable as adsorbents for biogas cleaning and upgrading.

Physisorption and Chemisorption in adsorption-based systems

As for absorption-based systems, it is possible as well to distinguish physisorption and chemisorption concerning adsorption-based systems.

In this case, physisorption occurs when the pollutant is bound to the surface of material due to intermolecular interactions, as Van der Waals forces, while chemisorption occurs when, due to the chemical composition of the gas stream and the presence of active sites on the sorbent surface, chemical reactions convert the pollutant other compounds, which are easier to bound to the sorbent surface.

Chemisorption allows to improve significantly the adsorption capacity of the sorbent (i.e. the mass of pollutant that can be adsorbed by one unit mass of sorbent), but it is strongly dependent on the amount of oxygen and humidity in the gas [43], Figure 3.2.

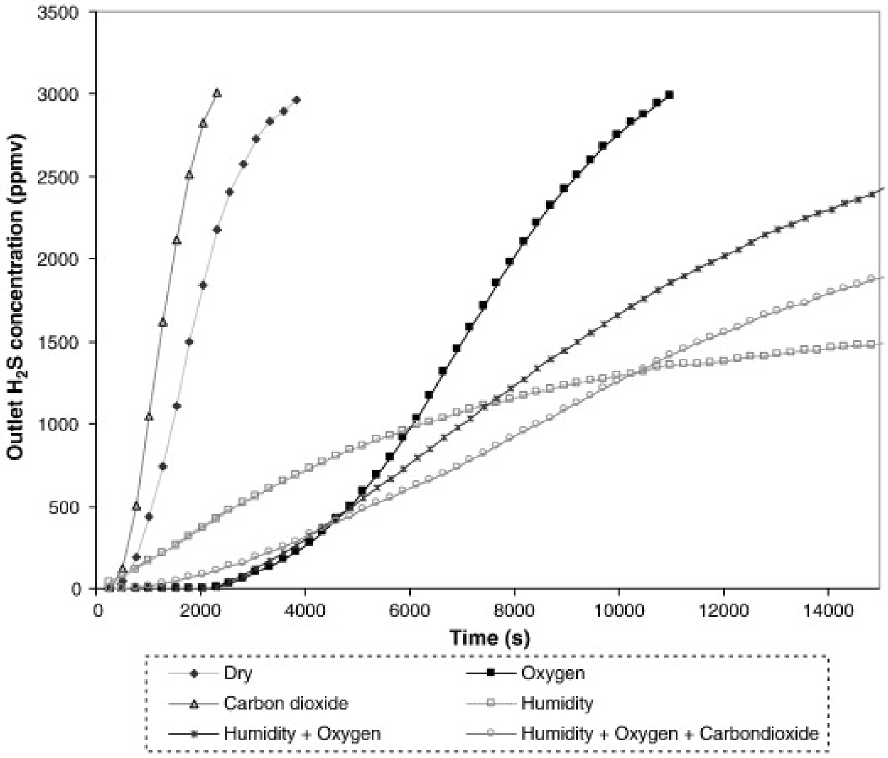

Figure 3.2: Sitthikhankaew et al., in 2014 analysed the effect of oxygen and humidity on KOH-impregnated activated carbons, their results shown a significant increase in activated carbons performance towards H2S adsorption, due to the deposition of elemental sulfur or the formation of sulfuric acid in the water film originated by humidity in the material's pores [43]

3.1.3 Cryogenic Technology

Cryogenic technologies are a relatively new field of research which exploits the different condensation temperature ranges of the different components in a biogas mixture to condense pollutants and freeze carbon dioxide, and easily remove them through gravity.
This procedure is currently exploited to upgrade biogas through CO_2 condensation (or brine), and potentially allow a direct production of liquefied biomethane [44].

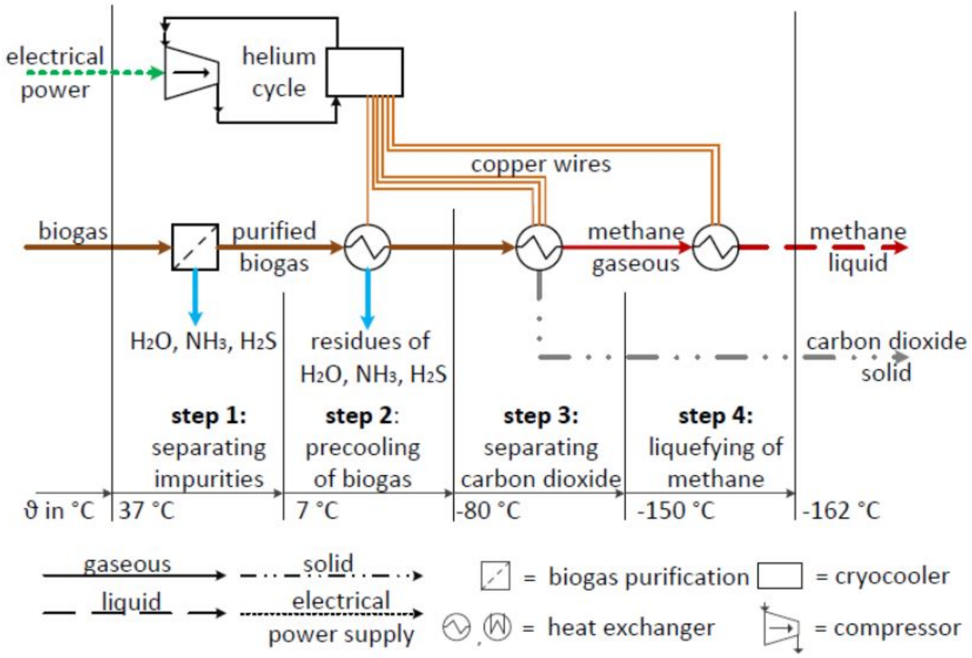

Figure 3.3: Schematic representation of a cryogenic separation system for LBM production [44]

The major positive aspects of cryogenic separation lie in the fact that high purity solid CO_2 is produced as byproduct, matching standards for industrial applications as process fluid or dry ice.
Since CO_2 plays an important role for biogas reforming in SOFCs (dry reforming), the economical advantages of solid carbon dioxide production may loose relevance for this type of applications if compared to biogas upgrading for grid injection or vehicle fuel applications.

3.2 Waste2Watt Project description

As anticipated in subsection 1.2.5, the goal of Waste2Watts is to develop cleaning systems for biogas applications to CHP production.
This work focuses on small scale units. In this context, biogas cleaning is performed through adsorption systems. Therefore, our goal lies in evaluating sorbent performances to select proper materials for the cleaning unit It is in this frame that the European projects “Waste2Watts” has been developed. The aim is the development of biogas-SOFC combined heat and power systems with minimal gas pre-processing, "focusing on low-cost biogas pollutant removal and optimal thermal

system integration" [1]. Politecnico di Torino, the Paul Scherrer Institute and the ENEA institute cooperated to analyse commercially available and innovative sorbent materials to provide information needed for the optimization of the cleaning stage of a small scale unit.

To properly plan the experimental campaign, a deep literature-based research has been coupled with PSI analysis on agro-biogas pollutants. The most abundant and most harmful pollutants in agro-biogas, which is the type of biogas that this experimental campaign focuses on, is mainly characterized by sulphur compounds. Therefore, the activity of the research groups is focused on:

- H_2S: Hydrogen Sulphide
- COS: Carbonyl Sulphide
- CH_4S: Methanethiol (or methyl mercaptan)
- DMS: Dimethyl Sulphide

The compounds of interest have then been divided among the partners. Politecnico di Torino focused its testing campaign on H_2S and will test CH_4 soon, ENEA tests were focused on COS and are now working on multi-contaminants, PSI is working on DMS and will test for multi-contaminants as well [45].

Chapter 4

Materials and Methods

4.1 Sorbent Specifications

Among the different types of adsorbent materials exploited in biogas cleaning applications (subsection 3.1.2), those tested in this project are a selection of commercially available and innovative ones obtained by taking direct contact with the suppliers. This samples, characterized by material type, are listed in Table 4.1 along with their supplier.

Name	Type	Supplier
ACTISORB S2	Metal Ox.	C & CS (DE) [46]
AIRPEL ULTRA D5	AC	AROL Energy (FR) [47]
AIRPEL ULTRA D5	AC	Desotec (BE) [48]
BIOCLEAN GAS GRANULAR	Metal Hydrox.	BIOCUSTOM SRL (IT) [49]
ENVIROCARB AP4-60	AC (non imp.)	CHEMVIRON (BE, US) [50]
ENVIROCARB STIX	AC	CHEMVIRON (BE, US) [50]
SOLCARB KS3	AC	CHEMVIRON (BE, US) [50]
NORIT RST3	AC	DOLDER (DE) [51]
NORIT RGM3	AC	DOLDER (DE) [51]
SULFATRAP R2F	Metal Ox.	SULFATRAP (US) [52]
SULFATRAP R2DB	Metal Ox.	SULFATRAP (US) [52]
SULFATRAP R5E	Metal Ox.	SULFATRAP (US) [52]
SULFATRAP R7H	Metal Ox.	SULFATRAP (US) [52]
SULFATRAP R7HB	Metal Ox.	SULFATRAP (US) [52]
SULFATRAP R8HB	AC	SULFATRAP (US) [52]
SULFATRAP R8C	AC	SULFATRAP (US) [52]

Table 4.1: Sorbents name, material type and suppliers, with reference to the company official web page.

This materials have been tested in the DISAT department of Politecnico di Torino to investigate their composition and their specific surface area. The first parameter is extremely relevant for those materials which perform chemisorption, as the reactions occur in specific active sites which can catalyse the reaction between the pollutant (e.g. H_2S) and a co-reactant, typically O_2 or H_2O (present as gas humidity). The specific surface area is a generally important parameter to evaluate the adsorption capacity, as a high BET-area leads to a higher interaction between the sorbent and the gas, and a higher amount of active sites (if the material is impregnated).

4.2 Sorbent Characterization

The BET analysis is a technique used to evaluate the specific surface area of a sorbent material through the analysis of the adsorption isotherms. The analysis requires a known amount of sorbent to be degases from any impurity and the evaluation of its adsorption behaviour.
Samples of each sorbent under analysis have been desorbed using a vacuum pump for three hours: initially the samples are heated using an electric heater and an insulation coating. The heating rate is 10řC/min and the target value is reach 200°C, to be kept for the remaining time. The schematic representation of the piping system is reported in Figure 4.1 as displayed by the software window. The green dots represent (D1, D5, D6) the opened valves connecting the sample tube to the vacuum line. A sample undergoing the procedure is shown in Figure 4.2.

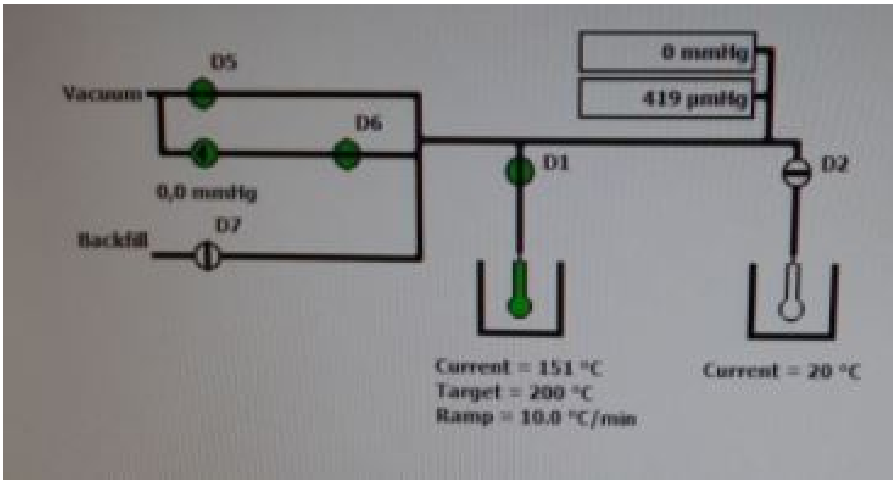

Current = 151 °C
Target = 200 °C
Ramp = 10.0 °C/min

Current = 20 °C

Figure 4.1: Schematic of the BET Analyzer lines in desorption mode, ASAP 2020 PLUS window.

Figure 4.2: Sample Tube heated in desorption mode. The sample is heated through an electric heater and covered in an insulation coating.

Once the sample is cooled to ambient temperature, it must be weighted to evaluate its mass after desorption occurred. The sample tube is then connected once more to the analyzer line whilst being submerged in a liquid nitrogen bath, which boils at 77 K at atmospheric pressure Figure 4.3. A stream of gaseous nitrogen is sent to the sample tube and its partial pressure is measured, allowing the evolution of the isotherm curve of adsorption.

Figure 4.3: Sample Tube submerged in a liquid nitrogen bath, testing mode

4.2.1 Results

The software ASAP 2020 Plus® generates results in text and Excel® files, which have further been elaborated to present the adsorption-desorption Langmuir isotherms, the specific area and the pore size distribution in the samples. The results of the analysis conducted at the DISAT laboratory at Politecnico di Torino have been compared to those conducted by the ENEA Institute and to literature references about similar sorbents, in material type and, eventually, supplier. Politecnico results are recorded in Table 4.2, alongside those found by ENEA tests or literature references on similar materials. These values are similar to both those found by the ENEA Institute over their samples and those found in literature over similar materials, with the maximum difference in the case of SulfaTrap R7H, characterized by a relative error of 162.12% with respect to a similar SulfaTrap sorbent analysed in literature. The minimum difference happens for the case of SulfaTrap R2DB, with a relative error of 0.65% with respect to a similar SulfaTrap sorbent analysed in the same article ([53]). If the comparison is restricted to ENEA tests only, the maximum relative error happens for the case of Solcarb KS3 (26.66%) and the minimum for the case of Norit RGM3 (4.88%). The final results of BET area are shown in Figure 4.4.

Additionally to the estimation of the specific surface area, the sorbents investigation also produces the adsorption-desorption curves in Figure 4.4. The specific surface area, the curves and the sorbent specifications on impregnation and producer declarations have been used to schedule the tests. As described in section 5.1, the chosen strategy is to start with those sorbents expected to have lower performances, thus to take advantage of the short duration of the first test to develop skills on the use of the test station before starting longer tests and tests on materials of particular interest (innovative ones).

Sorbent	Type	PoliTo $[m^2/g]$	ENEA/Lit. $[m^2/g]$	Ref.	Error [%]
ACTISORB S2	Metal Ox.	43.67	42.6	[54]	2.45
AIRPEL ULTRA D5 (AROL)	AC (imp.)	771.64	781.0	[55]	1.21
AIRPEL ULTRA D5 (DESOTEC)	AC (imp.)	697.45	//	//	11.98
BIOCLEAN GAS GRANULAR	Metal Hydrox.	130.66 - 133.66	N.F.	N.F.	N.F.
ENVIROCARB AP4-60	AC (non-imp.)	948.90	991	[56]	4.44
ENVIROCARB STIX	AC (imp.)	622.21	766	[56]	23.11
SOLCARB KS3	AC (imp.)	691.60	876	ENEA	26.66
NORIT RST3	AC (imp.)	743.13	1117	[39]	50.31
NORIT RGM3	AC (imp.)	1031.36	981	ENEA	4.88
SULFATRAP R2F	Metal Ox.	453.08	432	[53]	4.65
SULFATRAP R2DB	Metal Ox.	434.82	//	//	0.65
SULFATRAP R5E	Metal Ox.	160.74	N.F.		N.F.
SULFATRAP R7H	Metal Ox.	30.33	79.5	[53]	162.12
SULFATRAP R7HB	Metal Ox.	51.54	//	//	54.25
SULFATRAP R8HB	AC (imp.)	895.84	640	[53]	28.56
SULFATRAP R8C	AC (imp.)	687.17	//	//	6.86

Table 4.2: BET Analysis result: specific surface area evaluated, evaluated at DISAT laboratory at Politecnico di Torino in march 2021. Results compared to those from ENEA analysis on the same materials and literature reference to tests on same/similar materials.

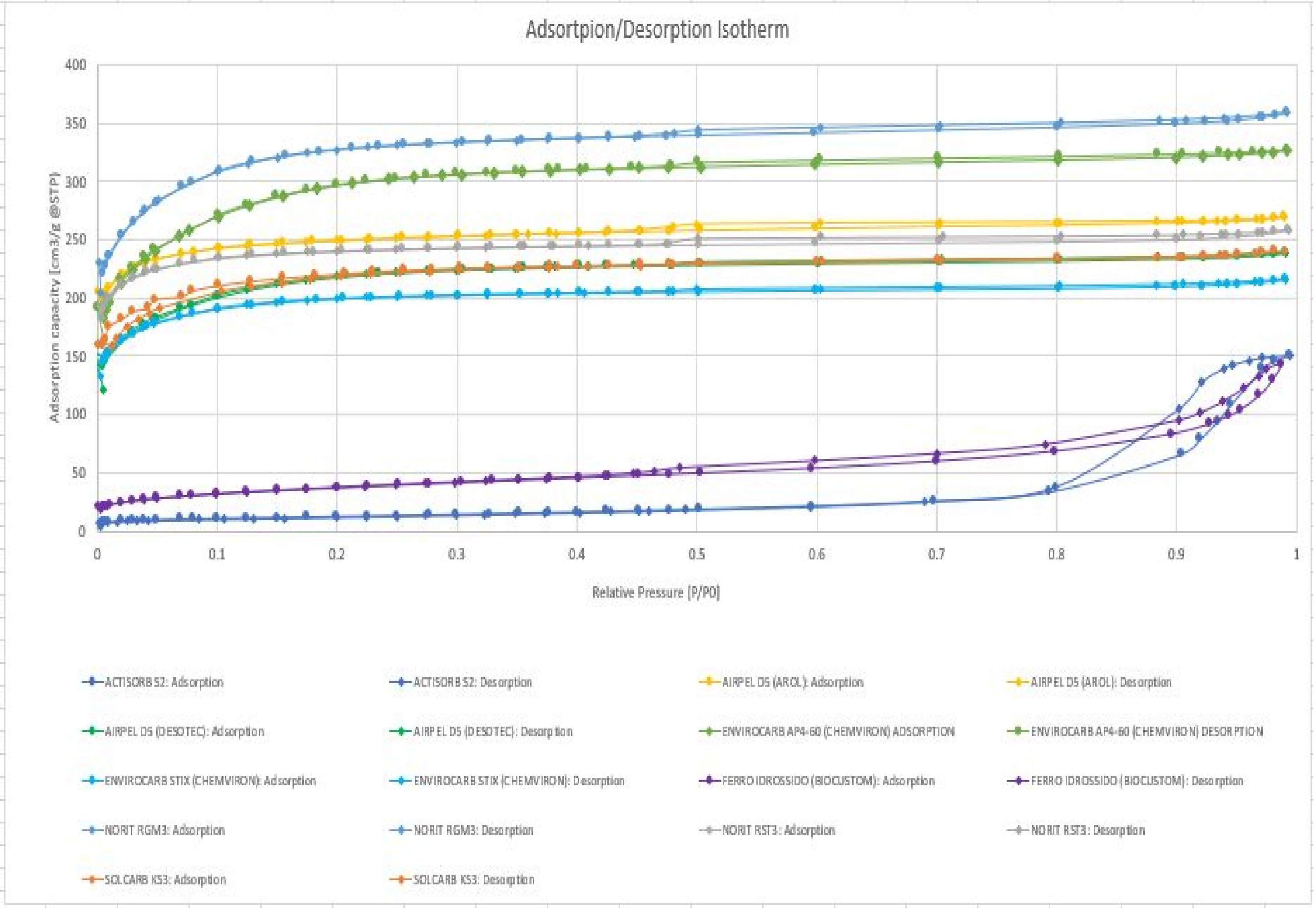

Figure 4.4: Adsorption-Desorption curves: BET Analysis from Politecnico di Torino. Adsorption Capacity for N_2 is expressed as standard volume per unit of mass.

4.3 Adsorption Analysis Campaign

The experimental set-up at Environment Park (Politecnico di Torino) works consists in a reactor bed, which contains the sorbets in granular form. A biogas-simulating gas flow is fed to the reactor using a set of Mass Flow Controllers (MFC), each one supplying one stream coming from a dedicated line (CO_2, CH_4, CH_4 + pollutant, and O_2). This procedure allows to control both total flow rate and the resulting composition.
Sorbent testing has been conducted using a different set of biogas compositions, both in term of methane and carbon dioxide abundances and in term of oxygen and humidity presence, which are fundamental for chemisorption. A realistic biogas composition has been simulated by mixing pure CH_4, pure CO_2, H_2S at 2000 ppm(v) in CH_4, and O_2.
Additionally, a bubbler able to saturate the stream has been implemented, in order to vary the stream humidity. The different streams are modified using a set of Mass Flow Controllers. All tests have been conducted with a specific Gas Hour Space Velocity (GHSV) and a specific L/D ratio. Table 4.3 contains data defining the reactor volume, the L/D ratio and the GHSV parameter. The latter is set as working parameter.

Parameter	Value	Unit	Found through:
Reactor Volume	0.024	dm^3	Geometry
L/D	3	-	Geometry Constrain
GHSV	1500	$[h^{-1}]$	Technological Constrain
Total Flow	610.27	$[Nml/min]$	above mentioned constrains
CO_2 content	50	%	screening condition
H_2S content	500	ppm(v)	screening condition

Table 4.3: L/D ratio is set to the minimum value of 3 to avoid the formation of preferential pathways. GHSV is set to 1500 as standard working parameter able to guarantee a sufficient residence time for the mass transfer to occur.

The L/D ratio is set to the minimum of 3, below this value it is highly probable that preferential pathways are formed in the pellet, allowing a faster flow that limits the interaction between the flow and the sorbent. This phenomenon does not affect the total sulphur that can be removed by the sorbet saturation, but the breakthrough is reached faster, thus affecting the adsorption capacity at saturation. The correlation between adsorption capacity and L/D ratio has been investigated and the results are displayed in Figure 4.5 [45].

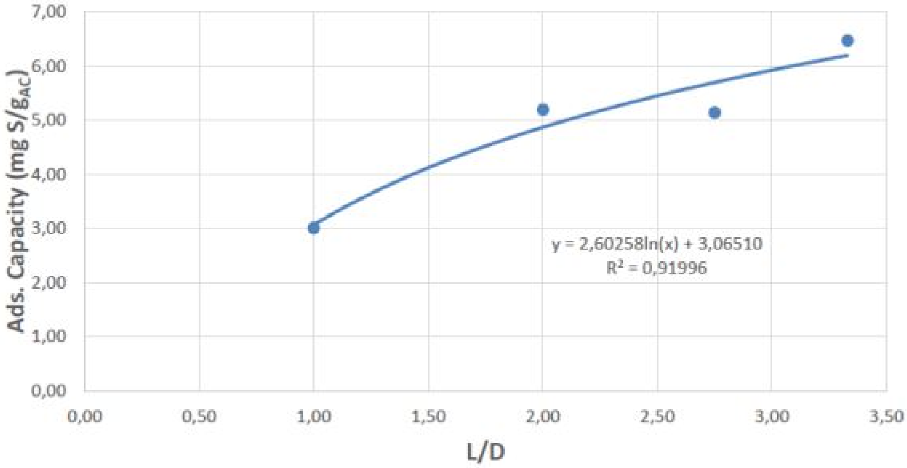

Figure 4.5: Correlation between L/D ratio and Adsorption Capacity [45]

Each line supplied by a MFC is separated into two different ones prior mixing. A set of lines is sent to a bubbler to be saturated in water (yellow arrow in Figure 4.7), humidity is later reduced by mixing it with the flow sent into the other set of lines (brown arrow in Figure 4.7).
Working with humidity sets specific constrains related to the solubility of H_2S and CO_2 in water, affecting both the flowrate and stream composition. Pure methane and oxygen are the only gasses sent to bubbler, sulphur-polluted methane and carbon dioxide are to be sent through the dry lines. Therefore, methane and sulphur content of the total stream becomes related to the level of humidity. This boundary, however, do not affect the humidity range of interest since, in realistic working conditions, the adsorption bed follows a dehumidification chiller to avoid the risk of pore clogging consequent to undesired condensation inside the bed.
Lastly, H_2S has a detrimental effect over the humidity detector. Therefore, it is needed to measure the humidity content of the stream by sending pure CH_4 to the bubbler and using pure CO_2 to represent the total dry flow of the test. Once the humidity is measured, the RH sensor is bypassed and the dry flow is separated into its single components (CO_2 and H_2S in CH_4.
The P&I Diagram of the Test Station is provided in Figure 4.6, detailed aspects of it are presented in detailed with the aid of the following pictures.

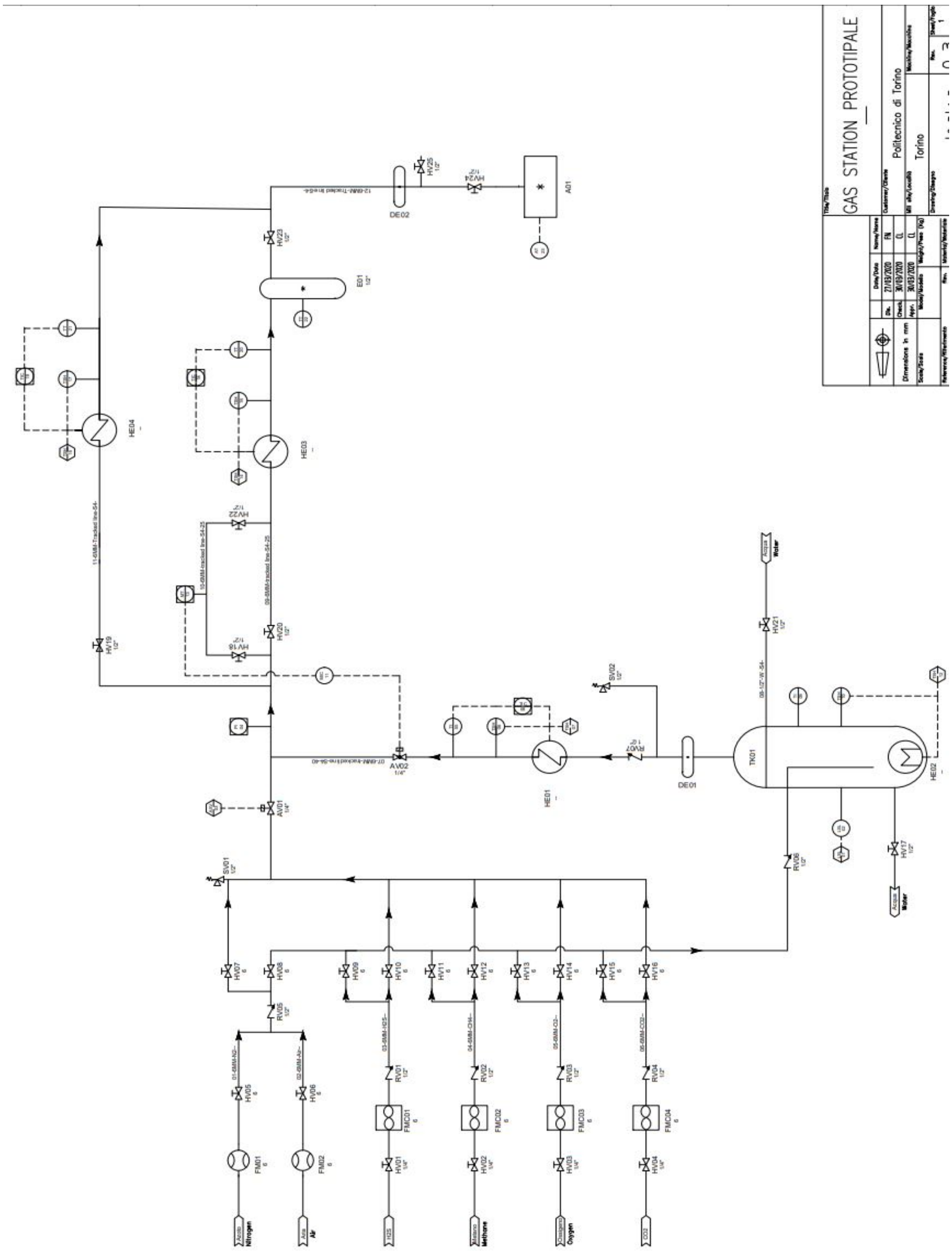

Figure 4.6: P&I diagram of the test station. It is possible to distinguish MFCs, the bubbler and the detectors for humidity and for hydrogen sulfide

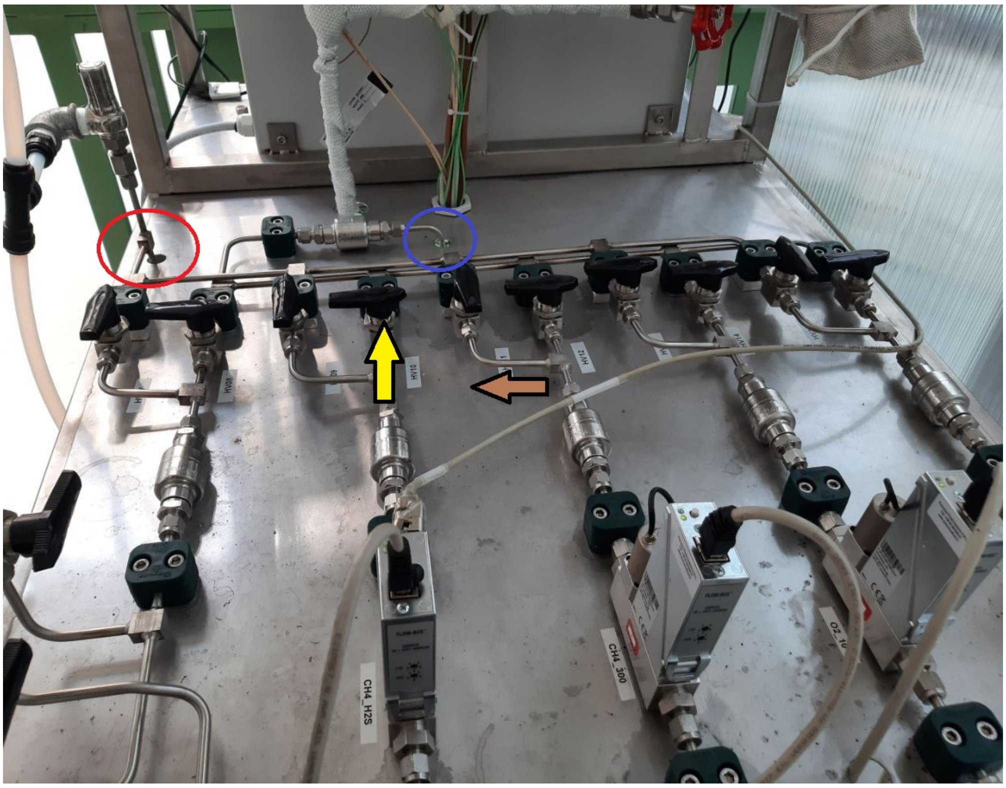

Figure 4.7: Test station gas lines. Each line is fed through a MFC and contains one specific flow. As shown by the arrows, each line is bifurcated. Following the main direction of the pipes (yellow arrow), the flows are merged and sent to the bubbler for humidification (blue circle), the alternative pathway (brown arrow) merges the flow and bypasses the bubbler (red circle).

The reactor used for the adsorption tests is cylindrical in shape, its precise geometry data are listed in Table 4.4, whilst the reactor, without coating, is shown in Figure 4.8. The reactor has its own insulated coating, a specific thermal resistance-based heating and a thermocouple used for temperature control.

L_{total} [cm]	D [cm]	$L_{sorbent, min}$ [cm]	L/D [-]
11.3	2.2	6.6	3.0 (lower bound)

Table 4.4: Reactor geometry data

Figure 4.8: Reactor without coating

In Figure 4.9 the full set of pipelines of the total flowrate is shown. During testing operations, the gas mixture coming from the bottom-left is sent directly to the reactor (here covered in its insulation coating), and then flows from the top-side of the reactor to the detector shown in Figure 4.10. The yellow arrow represents the flow direction of the by-pass line, used for flushes with CO_2 or air only. During normal operation, this line is closed and the gas flow is sent through the lower pipe (lower blue arrow) to enter the reactor (red arrow) and flow to the detector.
A second blue arrow shows the direction of the flow when it is needed to measure the humidity of the stream, since a humidity sensor is placed on top of this line. The three red valves in that region are used to define whether the flow is to be sent to the humidity sensor (control in tests with humidity, without the H_2S-containing stream) or to be sent directly to the reactor, bypassing the humidity sensor to avoid its sulphur poisoning (normal operation).

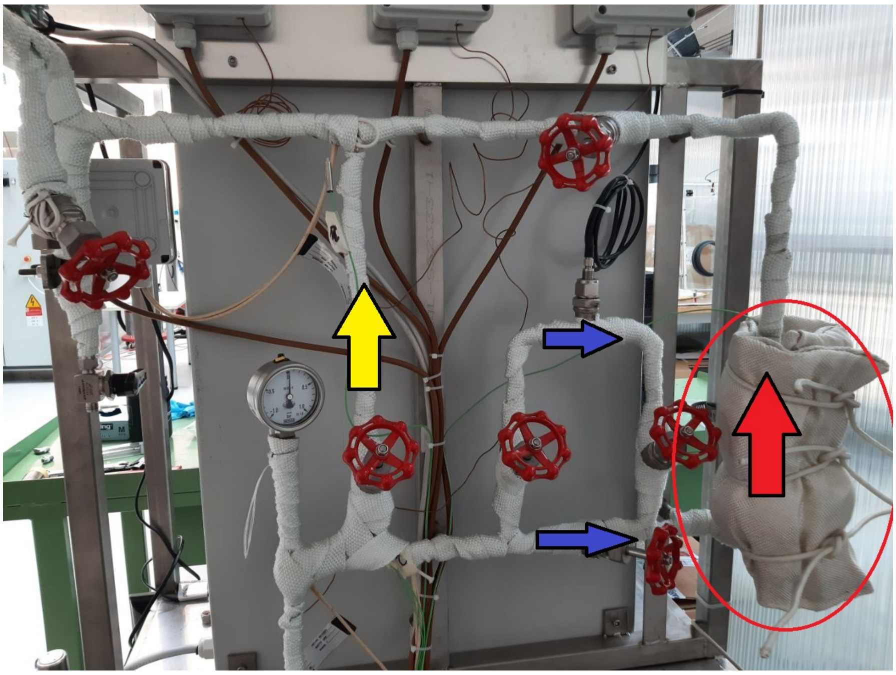

Figure 4.9: Top side of the test station: the reactor and humidity sensor are shown on the right

Finally, the vertical line on the left can bypass the reactor and send the flow directly to the detector. The outflow of the reactor is analyzed by a MECCOS sensor from Siegrist where the H_2S content is measured (instrument range 0-1000 ppm(v), error: 10% full scale, [57]) before being vented. As agreed by the Waste2Watts partners (PSI and ENEA), the breakthrough concentration is set to 1% of the inlet concentration for all tests.

Figure 4.10: H_2S Detector

In the Waste2Watt project all partners agreed to evaluate the breakthrough concentration as 1% of the feeding concentration. Therefore, the evaluation of the sorbent performances is performed by taking and recording the saturation measured concentration as reference. Once the test has ended, the time evolution of the concentration is exported as an Excel sheet and then read as a 2xN matrix in Matlab® (time and concentration, the detector time step is 1 second) to find the breakthrough as 1% of inlet value.
A more detailed description of the tests is reported in section 5.1.

Chapter 5

Experimental Activity

5.1 Screening Tests

The goal of the testing campaign is the preliminary screening of sorbents with a single pollutant to define which ones are suitable for the further steps of the analysis, as multi-pollutant cleaning.
As already said in section 3.2, Politecnico di Torino focused its initial tests on H_2S. Therefore, the first experiments were conducted in baseline concentration conditions: dry gas, absence of oxygen and a 50%-50% target for CH_4-CO_2 abundances.
As described in section 4.3, H_2S is provided by a CH_4 stream with a concentration of 2000 ppm(v) of pollutant. The required stream composition (H_2S and CH_4 content, given 50% CO_2) is reached through the ratio between the "pure" and the "polluted" methane streams. This procedure is done using an iterative method (The Excel®embedded function "target value search"). Therefore, these tests have been conducted in the conditions reported in the 'preliminary' column of Table 5.1. The 'O_2, RH' column contains information about the tests run in presence of oxygen and humidity after the preliminary screening has been completed.
The constrain on O_2 and RH is based on the need to maintain the mixture far from the flammability limits, which is not particularly compromising since, for chemisorption to occur, the oxygen content must be similar to the one of the pollutant (ideally stoichiometric ratio).
The constrain is RH is purely technological: since H_2S and CO_2 are soluble in water, the only stream that can be humidified in the bubbler is the one pure-methane one. Therefore, the maximum water vapour content of the stream is limited by the maximum and minimum content of H_2 and the CH_4 in the resulting mixture. Despite this, the project partners agreed to perform humidity-containing tests with a target RH value of 50%. Therefore, future tests will also vary the stream composition by lowering the CO_2 content and increasing the CH_4 one, thus

increasing the humidified flow across the bubbler to reach higher humidity content.

Species	Content (preliminary)	Content (O_2, RH)	unit
CO_2	50.00	50.00	% dry vol.
CH_4	49.95	49.45	% dry vol.
O_2	0	0.5	% dry vol.
H_2S	500	500	ppm(v)
H_2O (RH)	0	0-35	%(RH)

Table 5.1: Gas composition used for screening tests. Under the 'preliminary' column are reported the gas composition data used for dry screening in absence of oxygen, to assess the baseline performances of the sorbents. The column 'O_2, RH contains the data on gas composition for more realistic tests, in presence of oxygen and humidity.

Testing Procedure

The testing procedure consists in:

1. Loading the reactor with a weighted mass of sorbent such that the L/D ratio reaches at least the threshold level of 3, needed to avoid preferential pathways that would limit the interaction of the flow with the sorbent.

2. Opening the lines of those gasses that are to be used: CH_4, CO_2 and CH_4+H_2S are always used, O_2 is introduced after setting a preliminary test baseline with no oxygen and no humidity. Dry and wet lines are to be chosen in this step.

3. Selecting the opening degree of the valve connecting the wet lines to the bubbler for tests in presence of humidity (open=100%, closed=0%).
   Although the bubbler valve allows a range of opening degrees, it has been decided to use it only as a binary valve (open = 100%, close=0%). The RH degree is obtained by mass balance from the relative flow rates sent to the bubbler and those sent through the dry lines. The stream sent to the bubbler is completely saturated.

4. Operating the MFCs to generate the required flowrate of simulated biogas at the required conditions. If working with humidity:

   (a) The polluted stream is initially not used and the mixture is sent to the humidity detector to analyse the bubbler humidification efficiency.

   (b) The humidity reactor is bypassed and the polluted stream is included in the mixture. The previously analysed humidification efficiency is used to evaluate the RH of the new stream.

5. Analysing the H_2S concentration on the outflow of the reactor and defining the time steps in which the mixture has been sent to the reactor and the one in which the polluted stream has been removed from the mixture.

The absorption capacity is theoretically defined as the integral:

$$C_{\text{ads}} = \frac{Q * MM}{V_{\text{N}} * M_{\text{sorbent}}} \int_{t_1}^{t_2} y_0 - y(t), dt$$

- C_{ads} is the mass of H_2S adsorbed per unit of sorbent mass [%].

- Q = Total volumetric flowrate $[Nml/min]$.

- MM is the molar mass of the H_2S $[g/mol]$.

- V_{N} is the normal volume of 1 mole of ideal gas $(22.414 Nl/mol)$.

- M_{sorbent} is the overall sorbent mass $[g]$.

- y_0 is the inlet H_2S concentration and y(t) is the outlet H_2S concentration $[ppm(v)]$.

- t_1 and t_2 define the time interval of the test duration $[s]$.

The H_2S outlet concentration is measured and recorded by the NI SignalExpress-based software 'FlexLogger'. This software allows for a real-time display of the H_2S concentration measured by the detector in the forms of graph, clock hand and numerical value, as shown in Figure 5.1. The data are recorded and can be extracted as an Excel® file as a two-columns sheet containing both the H_2S concentration and the time evolution with a 1 second time-step. The Excel® sheet can be read through a Matlab® script, which results in a two-columns matrix containing the Finite Difference Approximation of the time evolution of the outlet concentration with a time-step of 1 second. The script analyse the matrix to identify the time instant at which the outlet concentration reached the breakthrough value. Lastly, the script plots the time evolution of the outlet concentration, as it is the case of the plots in section 5.3.

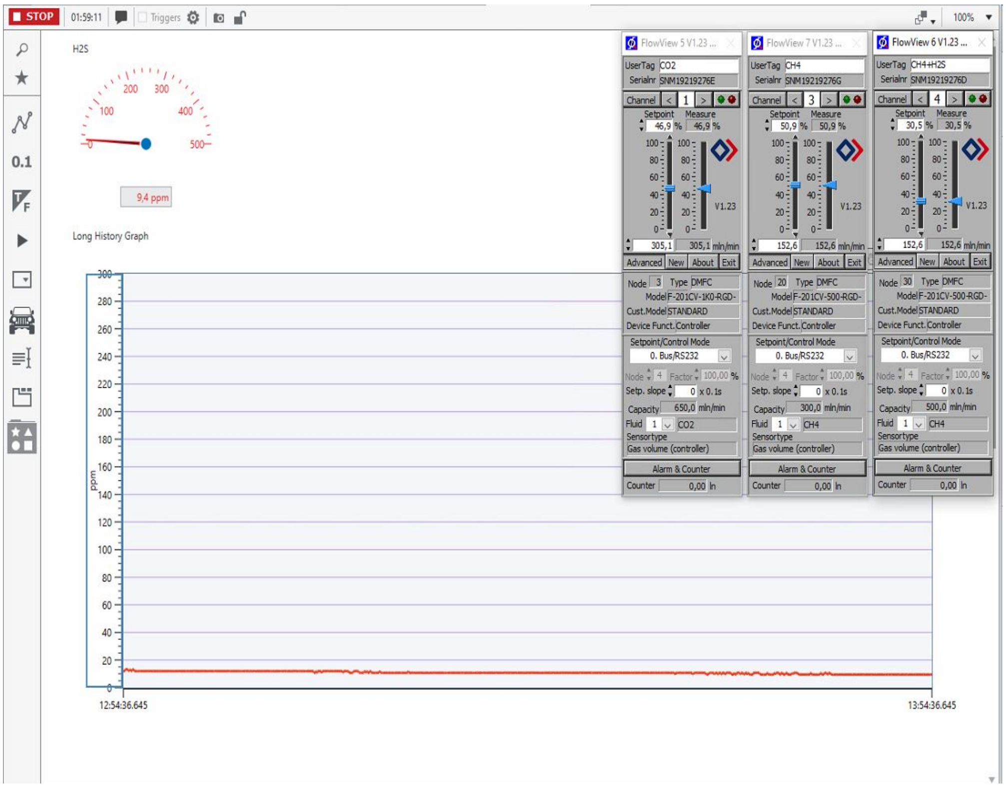

9,4 ppm

	FlowView 5 V1.23 ...	FlowView 7 V1.23 ...	FlowView 6 V1.23 ...
UserTag	CO2	CH4	CH4+H2S
Serialnr	SNM19219276E	SNM19219276G	SNM19219276D
Channel	1	3	4
Setpoint	46,9 %	50,9 %	30,5 %
Measure	46,9 %	50,9 %	30,5 %
Setpoint (mln/min)	305,1	152,6	152,6
Measure (mln/min)	305,1	152,6	152,6
Node	3	20	30
Type	DMFC	DMFC	DMFC
Model	F-201CV-1K0-RGD-	F-201CV-500-RGD-	F-201CV-500-RGD-
Cust.Model	STANDARD	STANDARD	STANDARD
Device Funct.	Controller	Controller	Controller
Setpoint/Control Mode	0. Bus/RS232	0. Bus/RS232	0. Bus/RS232
Node	4	4	4
Factor	100,00 %	100,00 %	100,00 %
Setp. slope	0 x 0.1s	0 x 0.1s	0 x 0.1s
Capacity	650,0 mln/min	300,0 mln/min	500,0 mln/min
Fluid	1 CO2	1 CH4	1 CH4
Sensortype	Gas volume (controller)	Gas volume (controller)	Gas volume (controller)
Counter	0,00 ln	0,00 ln	0,00 ln

Figure 5.1: Display of the FlexLogger measurement in real time (red line on graph). The three windows on the top right corner are the user interface to the MFC communication systems through which it is possible to define the flowrate of each gas.

The strategy for the testing campaign was to start with the sorbents which, due to the specific surface area, composition and the company reputation, are expected to have lower performances, to rapidly analyse the test station working before

proceeding with longer tests and with tests involving oxygen and humidity. For example, the first sorbent chosen was Envirocarb STIX, an activated carbon suitable for working far from RH saturation, according to the supplier's specifications. This characteristic makes it suitable for initial dry tests.
The results of the tests are reported in Table 5.3.

5.2 Tests with Oxygen Traces

The presence of oxygen traces in real biogas is interesting to evaluate the possibility to remove pollutants through chemisorption. Its origin in real biogas streams can depend on the non-ideal pipeline sealing, and therefore by air leaking into the stream.
Testing the effect of oxygen traces required an additional safety measure, which is the guarantee that the CH_4-O_2 mixture can never enter the flammability range. Therefore, the MFC controlling the oxygen stream is designed to have a flow range two orders of magnitude lower than the ones for methane and carbon dioxide.
The oxygen-containing mix is defined by keeping the same amount of CH_4 (50% vol), and a fixed 0.5% O_2. Once again, the CO_2 is defined by subtraction of all the other flows from the total one, which remains fixed at 610.4 Nml/min, and the CH_4 stream is the sum of a pure-methane stream and a stream with a known concentration of pollutant. The ratio of the streams is found through a "target value search" (embedded Excel®function) to reach the desired pollutant concentration. The final result of this analysis is the set of flow rates in Table 5.2.

Stream	Flow rate [Nml/min]
CO_2	302.1
CH_4	152.6
CH_4 + H_2S	152.6
O_2	3.1

Table 5.2: Tests with Oxygen traces (0.5% O_2)

5.3 Results and Comments

The following section presents the results of the testing campaign. The performance evaluation is expressed in term of breakthrough time, adsorption capacity at breakthrough and, if possible, adsorption capacity at saturation. Reaching complete saturation is interesting to develop a complete screening of the sorbents, but the key aspect of interest, at industrial viewpoint, is the breakthrough. Therefore, tests considered to be lasting too long have been interrupted before reaching complete saturation. This choice has been made to avoid excessive gas consumption and to avoid delays in the experimental campaign. This is the case of SulfaTrap R7HB and Norit RGM3 when tested with O_2 and O_2 + humidity, due to the long test duration. The same criteria has been applied to a shorter Norit RGM3 test dry test in absence of O_2 (rep. II), assessing the breakthrough time and adsorption capacity without excessive gas consumption. Finally, BioClean Gas Granular showed an instantaneous spike at the output at the beginning of the test, therefore its breakthrough is considered to be null.

Further details can be found in comments associated to Figure 5.4, Figure 5.5 and Figure 5.6.

Sorbent Name	Sorbent Mass [g]	Cads (BT) [%]	Cads (saturation) [%]	BT Time [h]
Envirocarb STIX	17.81	0.44	1.08	2.79
Envirocarb STIX (rep. I)	17.78	0.47	1.35	3.02
Envirocarb STIX (rep. II)	17.81	0.59	2.26	3.09
Envirocarb AP4-60	12.90	-	0.11	-
SulfaTrap R7HB	37.38	14.02	-	130.75
Norit RGM3	11.20	2.30	3.95	9.18
Norit RGM3 (rep. I)	14.04	2.74	4.29	13.83
Norit RGM3 (rep. II)	14.20	3.29	-	13.31
Norit RGM3 (O_2, rep. III)	14.20	5.92	-	30.25
Norit RGM3 (O_2, H_2O, rep. IV)	14.20	22.81	-	0.39
BioClean Gas Granular	16.97	-	-	0

Table 5.3: Screening test results in term of breakthrough time and adsorption capacity

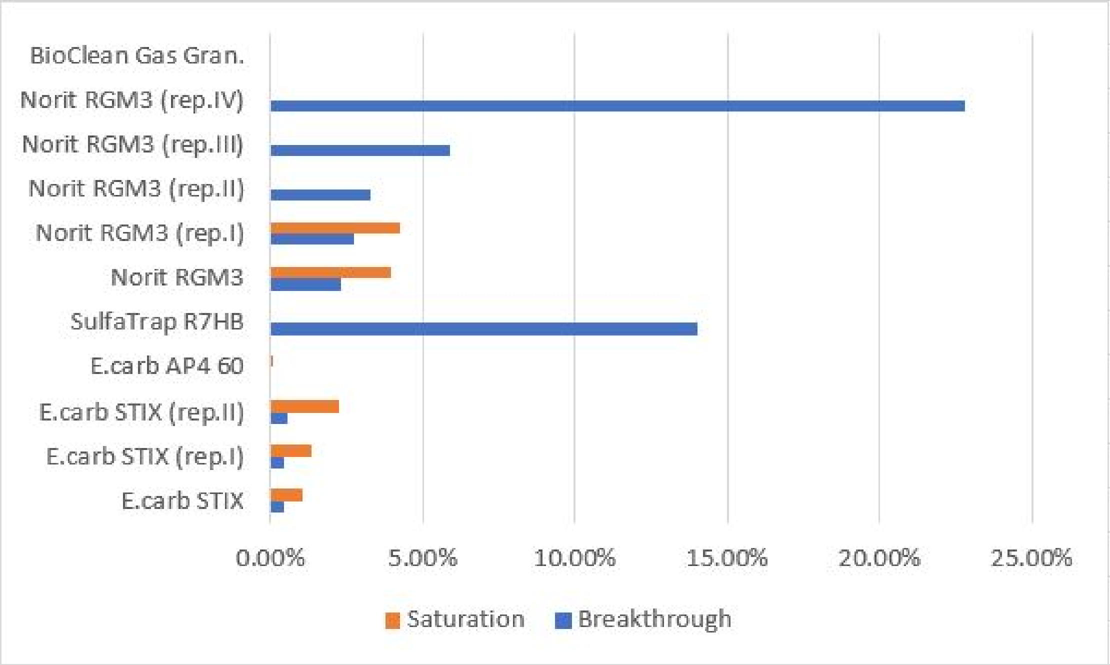

Figure 5.2: Graphical representation of the adsorption capacity of the sorbents at breakthrough (from Table 5.3)

According to the test results, shown in Table 5.3 and Figure 5.2, SulfaTrap R7HB is currently the sorbent characterized by the highest adsorption capacity and the longest breakthrough time in dry, anhydrous conditions. Conversely, the non-impregnated activated carbon Envirocarb AP4-60 proved to be significantly less performing than the other sorbents, showing an initial outlet concentration immediately growing with an exponential behaviour without a significant breakthrough time.

The impregnated AC Norit RGM3 shows both the adsorption capacity and the breakthrough time higher than the ones of the other impregnated AC (Envirocarb STIX) by one order of magnitude. Its performances also showed a considerable improvement when working with O_2 and, since Envirocarb STIX is also an impregnated AC, its performances are expected to improve those conditions as well.

Conversely, Envirocarb AP4-60, which is a non-impregnated AC, is not expected to gain any significant improvement from the presence of oxygen. Therefore, it might be not of interest of this project to perform further tests on Envirocarb AP4-60.

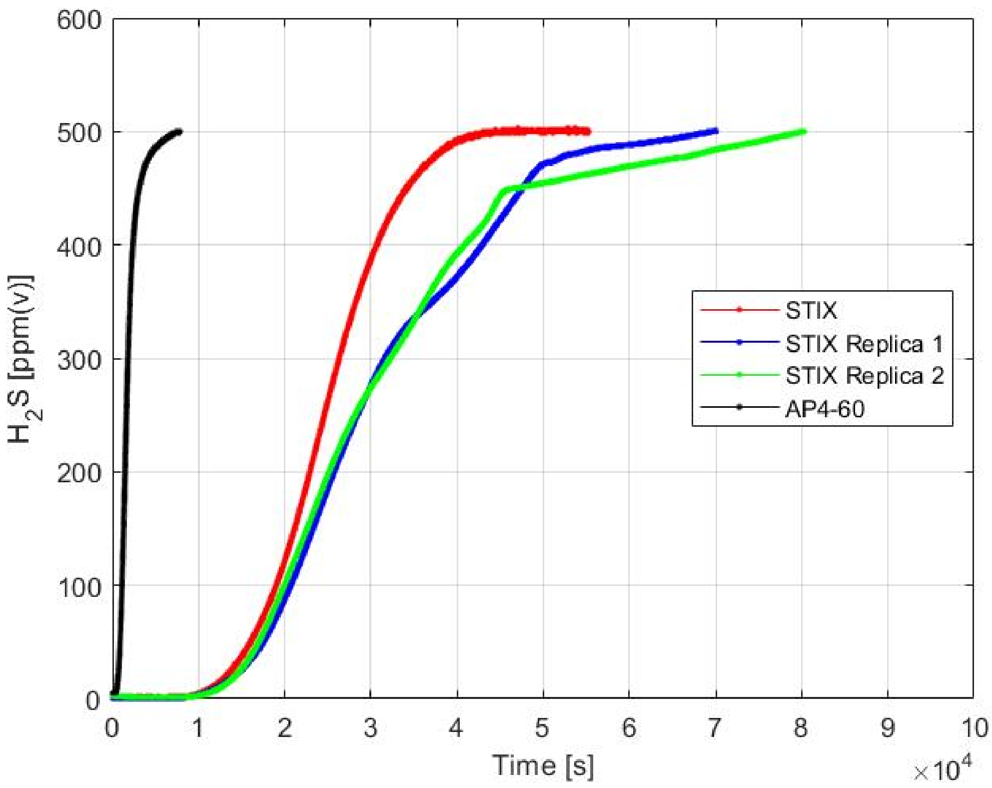

Figure 5.3: Envirocarb ACs, STIX repetitions and AP4-60, adsorption profile

Figure 5.3 contains the adsorption profiles of Envirocarb ACs. The three tests of Envirocarb STIX show similar behaviour (and comparable breakthrough times), but the first one is significantly smoother than the others. Therefore, it is taken as reference to compare the difference in adsorption capacity for each replica. The replicas were done right after the first test and between one test and the other a short flush with air was done to clean the H2S sensor. The graph underlines once again the difference in performances between STIX and AP4-60.

Sorbent	Cads BT	Cads sat.	Rel. error BT[%]	Rel. error sat. [%]
STIX	0.436	1.080	Ref. Val.	Ref. Val.
STIX (Rep. 1)	0.437	1.352	8.6	25.2
STIX (Rep. 2)	0.590	2.262	35.3	109.4

Table 5.4: Envirocarb STIX replicas results comparison. Relative error refers to the first STIX test.

The adsorption capacity of Envirocarb STIX are listed in Table 5.4. The resulting comparison of the replicas with one another, taking the first test as reference, underlines that the adsorption capacity varies strongly in the last test, characterised by a non smooth profile in the exponential growth. It has been suggested that the H_2S sensor was affected by long, repetitive, exposures to the pollutant. To mitigate this phenomenon, the duration of air flushes has been extended.

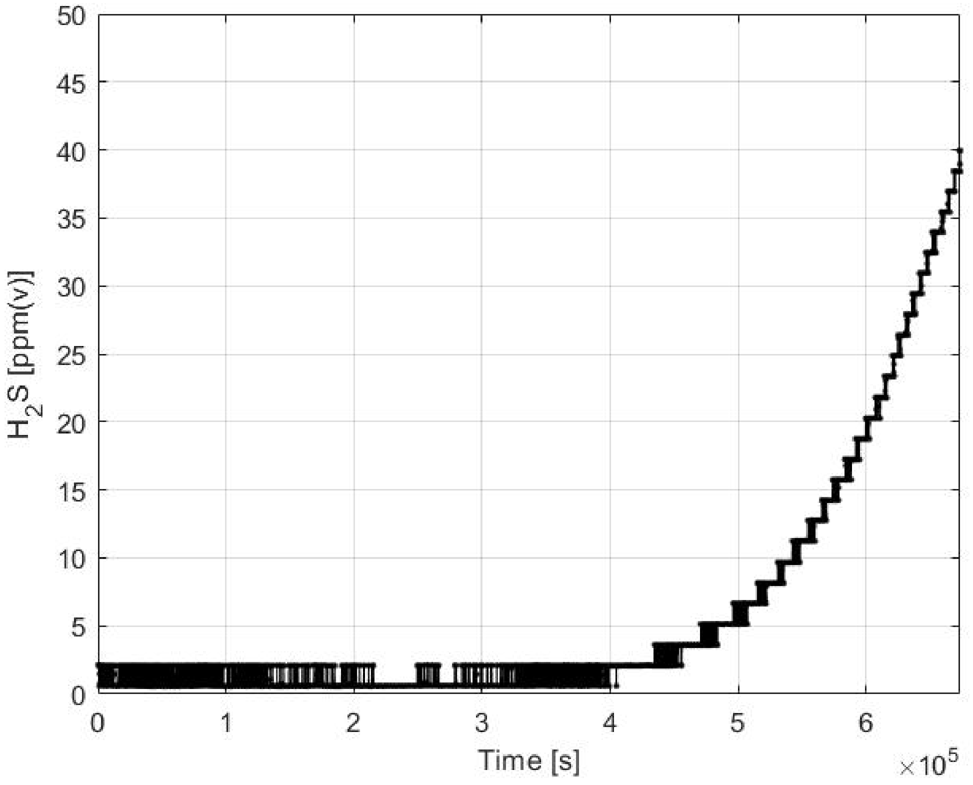

Figure 5.4: SulfaTrap R7HB adsorption profile

Figure 5.4 shows the adsorption curve of SulfaTrap R7HB, a metal oxide coming from a well-known supplier on the market. It was expected to have significantly valid performances and the test result confirmed such assumption. SulfaTrap R7HB test was prematurely stopped after 10 days of testing, as the breakthrough time has already been reached but not the saturation. This choice was made to save time and gas for the following experiments.

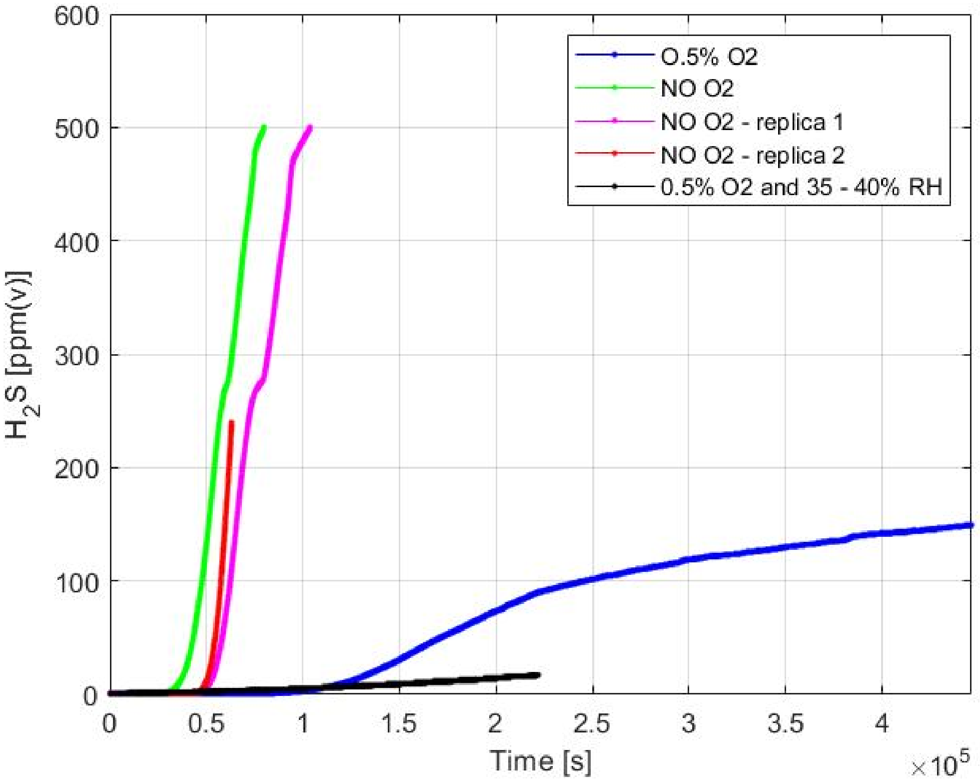

Figure 5.5: Norit RGM3 replicas adsorption profile

Figure 5.5 shows the adsorption profiles of the tests on the impregnate AC Norit RGM3. In dry, anhydrous conditions, its performances are better than both the non-impregnated AC Envirocarb AP4-60 and the impregnated AC Envirocarb STIX, as reported in Table 5.3. Additionally, its performances improved significantly in presence of oxygen (as expected from an impregnated AC) and humidity. The presence of O_2 caused both an increased adsorption capacity and a longer breakthrough time. The addition of water vapour to the stream caused a considerably slower growth in the adsorption curve but, according to Table 5.3, the breakthrough time was considerably lowered, even if compared to dry tests. This result is unexpected, hence future tests in the same conditions will be needed to understand if this phenomenon is characterised by the presence of moisture or if it was the consequence of other factors.

As reported in Table 5.3, the masses of the first test (green line) and the second test (replica 1, purple line) differ by 25.4%, resulting in a "delay effect" of one profile compared to the other. All of the subsequent tests were done using the same mass of the second test.

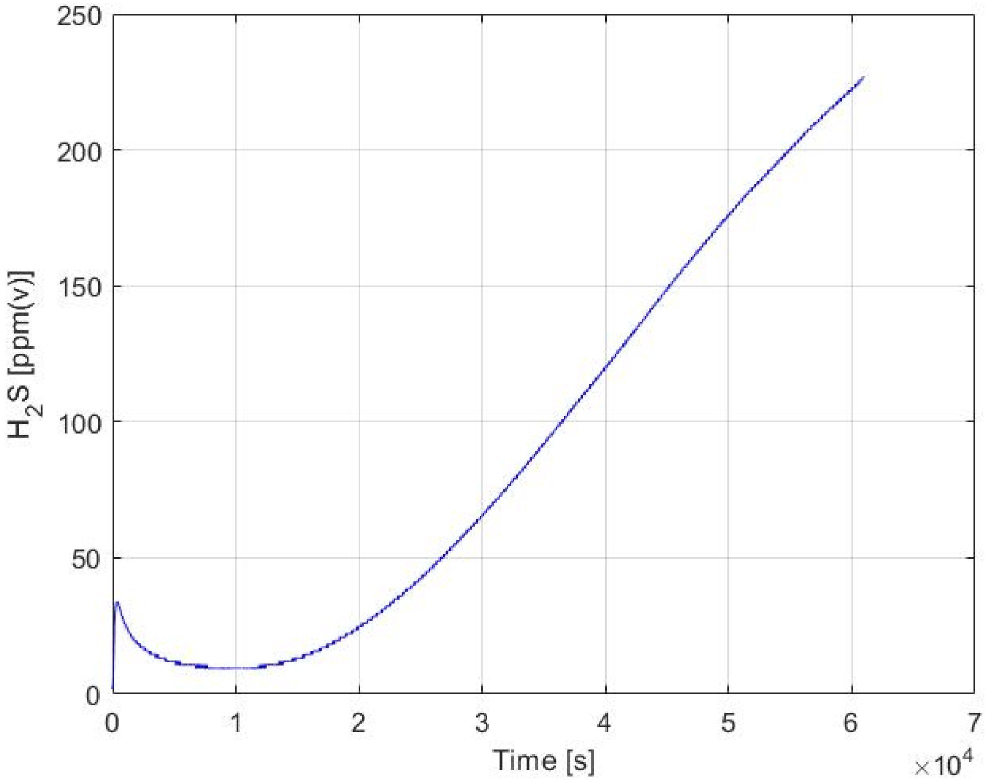

Figure 5.6: BioClean Gas Granular adsorption curve

Figure 5.6 shows the adsorption curve of the BioClean Gas Granular sorbent tested in dry, anhydrous conditions. As the curve highlights, the outlet concentration immediately reaches an initial peak that stabilizes as a local minimum before entering the exponential growth. The height of the peak causes the breakthrough time to be instantaneous, it is therefore mandatory to explore this phenomenon further in order to understand its causes and possible solutions.

5.3.1 Future Tests Planning

Future tests will carry on the investigation of the effects of oxygen and humidity compared to dry, anhydrous conditions.
Sorbents not yet tested and sorbents to test for more replicas are listed in Table 5.5. The table contains notes on their main characteristics and information given by the supplier or deduced from the material characterization analysis Table 5.5.
A deep focus will be dedicated to innovative sorbents which can be regenerated. To analyse the detrimental effect of the regeneration process on the sorbent performances it has been planned to analyse samples of expired sorbent before and after the regeneration and to test them to analyse the new performances.
The final goal is to map sorbents in presence of oxygen and humidity. An additional focus will be dedicated to materials of interest, as innovative ones, those able to be regenerated, and those that performed considerably well in the testing campaign. These sorbents will undergo a post-mortem analysis to correlate the adsorption dynamic of the sorbent to its structural changes.

Sorbents	Notes
Actisorb S2	Metal based sorbent No supplier-given data concerning RH and O2 Low BET-adsorption profile (DISAT analysis)
Solcarb KS3	Impregnated AC Not suitable for saturation conditions Suitable for thiols and organic sulphides
SulfaTrap R2F, R5, R8	Metal based sorbents Expected to be highly performing
BioClean Gas Granular	Metal based No supplier-given data concerning RH Low BET-adsorption profile (DISAT analysis) Innovative material, able to be regenerated Able to be disposed of by inserting it into the digeste
NORIT RST3	Impregnated AC, It can be regenerated using water
Airpel Ultra D5 (Arol Energy, Desotec)	Low BET-adsorption profile (DISAT analysis) RH range: 75 – 95%

Table 5.5: Sorbent materials to be tested and notes on their main characteristics

Finally, since some sorbents are able to be regenerated, it is interesting to analyse the evolution of the performances after each regeneration cycle. This process, done after the post post-mortem analysis, can be done according to the sorbents specifications defined by the suppliers (Table 5.6).

Sorbents	Regeneration Process
BioClean Gas Granular	Air (exposure)
Norit RST	Water (must be dried before re-use)

Table 5.6: Regeneration process suggested by the respective suppliers

After the regeneration process is completed, the sorbents can be further characterised through BET and XRD analysis and tested. The evolution of the sorbent performances with each cycle, coupled with the structural and composition modifications, will define the effectiveness of the regeneration process and the correlation between the material characteristics and the resulting performances.

Bibliography

[1] *DESCRIPTION | waste2watts-project.* URL: `https://waste2watts-project.net/description/` (visited on 06/05/2021) (cit. on pp. i, 10, 22).

[2] *EU climate action and the European Green Deal | Climate Action.* URL: `https://ec.europa.eu/clima/policies/eu-climate-action` (visited on 06/05/2021) (cit. on p. 1).

[3] Evelyne Monfet, Geneviève Aubry, and Antonio Avalos Ramirez. «Nutrient removal and recovery from digestate: a review of the technology». In: *Biofuels* 9.2 (Mar. 2018), pp. 247–262. ISSN: 1759-7269. DOI: `10.1080/17597269.2017.1336348`. URL: `https://www.tandfonline.com/doi/full/10.1080/17597269.2017.1336348` (cit. on p. 2).

[4] *Outlook for biogas and Prospects for organic growth World Energy Outlook Special Report biomethane.* Tech. rep. (cit. on pp. 2, 4).

[5] *Bioenergy Europe.* Tech. rep. 2021. URL: `www.bioenergyeurope.org` (cit. on pp. 2, 3).

[6] Nigel Bruce, Dan Pope, Eva Rehfuess, Kalpana Balakrishnan, Heather Adair-Rohani, and Carlos Dora. «WHO indoor air quality guidelines on household fuel combustion: Strategy implications of new evidence on interventions and exposure-risk functions». In: *Atmospheric Environment* 106 (Apr. 2015), pp. 451–457. ISSN: 18732844. DOI: `10.1016/j.atmosenv.2014.08.064` (cit. on p. 4).

[7] S. Venkata Mohan. *Harnessing of biohydrogen from wastewater treatment using mixed fermentative consortia: Process evaluation towards optimization.* Sept. 2009. DOI: `10.1016/j.ijhydene.2009.05.062` (cit. on p. 4).

[8] Shikha Dahiya, A. Naresh Kumar, J. Shanthi Sravan, Sulogna Chatterjee, Omprakash Sarkar, and S. Venkata Mohan. *Food waste biorefinery: Sustainable strategy for circular bioeconomy.* Jan. 2018. DOI: `10.1016/j.biortech.2017.07.176` (cit. on p. 6).

[9] M. Santarelli, S. Barra, F. Sagnelli, and P. Zitella. «Biomass-to-electricity: Analysis and optimization of the complete pathway steam explosion - enzymatic hydrolysis - anaerobic digestion with ICE vs SOFC as biogas users». In: *Bioresource Technology* 123 (Nov. 2012), pp. 430–438. ISSN: 09608524. DOI: `10.1016/j.biortech.2012.07.021` (cit. on p. 8).

[10] Andrea Lanzini and Pierluigi Leone. «Experimental investigation of direct internal reforming of biogas in solid oxide fuel cells». In: *International Journal of Hydrogen Energy* 35.6 (Mar. 2010), pp. 2463–2476. ISSN: 03603199. DOI: `10.1016/j.ijhydene.2009.12.146` (cit. on p. 8).

[11] GE Power. *Jenbacher Type 6 Specifications*. 2009 (cit. on p. 8).

[12] GE Energy. *Jenbacher type 3*. 2010. URL: `https://www.ge-distributedpower.com/products/power-generation/jenbacher-type-3-633-1063kw` (cit. on p. 8).

[13] Richard Van Schie and Bootham Lane. «Jenbacher type 4». In: (2003), pp. 4–5. URL: `https://www.ge-distributedpower.com/products/power-generation/up-to-5mw/jenbacher-type-4` (cit. on p. 8).

[14] A. Baldinelli, L. Barelli, and G. Bidini. «On the feasibility of on-farm biogas-to-electricity conversion: To what extent is solid oxide fuel cells durability a threat to break even the initial investment?» In: *International Journal of Hydrogen Energy* 43.35 (Aug. 2018), pp. 16971–16985. ISSN: 03603199. DOI: `10.1016/j.ijhydene.2018.02.031` (cit. on p. 8).

[15] M. Gandiglio, D. Drago, and M. Santarelli. «Techno-economic Analysis of a Solid Oxide Fuel Cell Installation in a Biogas Plant Fed by Agricultural Residues and Comparison with Alternative Biogas Exploitation Paths». In: *Energy Procedia*. Vol. 101. Elsevier Ltd, Nov. 2016, pp. 1002–1009. DOI: `10.1016/j.egypro.2016.11.127` (cit. on p. 8).

[16] Henry Wasajja, Ralph E.F. Lindeboom, Jules B. van Lier, and P. V. Aravind. *Techno-economic review of biogas cleaning technologies for small scale off-grid solid oxide fuel cell applications*. 2020. DOI: `10.1016/j.fuproc.2019.106215` (cit. on pp. 7, 13, 14).

[17] Eiji Sasaoka, Shigeru Hirano, Shigeaki Kasaoka, and Yusaku Sakata. *Characterization of Reaction between Zinc Oxide and Hydrogen Sulfide*. Tech. rep. 1994, pp. 1100–1105. URL: `https://pubs.acs.org/sharingguidelines` (cit. on p. 8).

[18] *DESCRIPTION | waste2watts-project*. URL: `https://waste2watts-project.net/description/` (visited on 06/05/2021) (cit. on p. 8).

[19] M. Santarelli et al. «Carbon recovery and re-utilization (CRR) from the exhaust of a solid oxide fuel cell (SOFC): Analysis through a proof-of-concept». In: *Journal of CO2 Utilization* 18 (2017). ISSN: 22129820. DOI: `10.1016/j.jcou.2017.01.014` (cit. on p. 8).

[20] *DEMOnstration of large SOFC system fed with biogas from WWTP | DEMOSOFC Project | H2020 | CORDIS | European Commission*. URL: `https://cordis.europa.eu/project/id/671470` (visited on 06/05/2021) (cit. on p. 8).

[21] *Deliverable "DEMOnstration of large SOFC system fed with biogas from WWTP"*. URL: `http://www.demosofc.eu/wp-content/uploads/2017/10/SOFC-based-CHP-market-potential-analysis.pdf` (visited on 06/05/2021) (cit. on p. 8).

[22] Marta Gandiglio, Andrea Lanzini, Massimo Santarelli, Marco Acri, Tuomas Hakala, and Markus Rautanen. «Results from an industrial size biogas-fed SOFC plant (the DEMOSOFC project)». In: *International Journal of Hydrogen Energy* 45.8 (2020). ISSN: 03603199. DOI: `10.1016/j.ijhydene.2019.08.022` (cit. on p. 9).

[23] *Home Page | Bio-komp.com*. URL: `http://www.bio-komp.com/index.php` (visited on 06/10/2021) (cit. on p. 10).

[24] Dionissios D. Papadias, Shabbir Ahmed, and Romesh Kumar. «Fuel quality issues with biogas energy - An economic analysis for a stationary fuel cell system». In: *Energy* 44.1 (2012). ISSN: 03605442. DOI: `10.1016/j.energy.2012.06.031` (cit. on pp. 11, 12, 14).

[25] Mona Arnold, Torsti Loikkanen, Jari Konttinen, Jukka Hyvönen, Laura Ruotsalainen, Kirsi Tuominen, Mika Waris, and Veli-Pekka Hyttinen. *VTT RESEARCH NOTES 2496 VTT CREATES BUSINESS FROM TECHNOLOGY Technologyandmarketforesight • Strategicresearch • Productandservicedevelopment • IPRandlic • Assessments,testing,inspection,certification • Technologyandinnovationmanagement • Techn Reduction and monitoring of biogas trace compounds VTT Tiedotteita-Research Notes*. ISBN: 978-951-38-7314-1 (cit. on p. 13).

[26] Weiwei Du and Wayne Parker. «Modeling volatile organic sulfur compounds in mesophilic and thermophilic anaerobic digestion of methionine». In: *Water Research* 46.2 (2012). ISSN: 18792448. DOI: `10.1016/j.watres.2011.11.043` (cit. on p. 13).

[27] Dimitrios K. Niakolas. «Sulfur poisoning of Ni-based anodes for Solid Oxide Fuel Cells in H/C-based fuels». In: *Applied Catalysis A: General* 486 (Sept. 2014), pp. 123–142. ISSN: 0926-860X. DOI: `10.1016/J.APCATA.2014.08.015` (cit. on p. 13).

[28] Hossein Madi, Andrea Lanzini, Stefan Diethelm, Davide Papurello, Jan Van Herle, Matteo Lualdi, Jørgen Gutzon Larsen, and Massimo Santarelli. «Solid oxide fuel cell anode degradation by the effect of siloxanes». In: *Journal of Power Sources* 279 (Apr. 2015), pp. 460–471. ISSN: 0378-7753. DOI: `10.1016/J.JPOWSOUR.2015.01.053` (cit. on p. 14).

[29] K. Haga, S. Adachi, Y. Shiratori, K. Itoh, and K. Sasaki. «Poisoning of SOFC anodes by various fuel impurities». In: *Solid State Ionics* 179.27-32 (2008). ISSN: 01672738. DOI: `10.1016/j.ssi.2008.02.062` (cit. on p. 14).

[30] R. J. Spiegel and J. L. Preston. «Test results for fuel cell operation on anaerobic digester gas». In: *Journal of Power Sources* 86.1 (2000). ISSN: 03787753. DOI: `10.1016/S0378-7753(99)00461-9` (cit. on p. 14).

[31] Andrea Lanzini, Hossein Madi, Vitaliano Chiodo, Davide Papurello, Susanna Maisano, Massimo Santarelli, and Jan Van herle. *Dealing with fuel contaminants in biogas-fed solid oxide fuel cell (SOFC) and molten carbonate fuel cell (MCFC) plants: Degradation of catalytic and electro-catalytic active surfaces and related gas purification methods.* Tech. rep. 2017. DOI: `10.1016/j.pecs.2017.04.002` (cit. on p. 15).

[32] Luong N. Nguyen et al. *Biomethane production from anaerobic co-digestion at wastewater treatment plants: A critical review on development and innovations in biogas upgrading techniques.* 2021. DOI: `10.1016/j.scitotenv.2020.142753` (cit. on pp. 16–18).

[33] Irini Angelidaki, Laura Treu, Panagiotis Tsapekos, Gang Luo, Stefano Campanaro, Henrik Wenzel, and Panagiotis G. Kougias. *Biogas upgrading and utilization: Current status and perspectives.* 2018. DOI: `10.1016/j.biotechadv.2018.01.011` (cit. on pp. 16–18).

[34] Qie Sun, Hailong Li, Jinying Yan, Longcheng Liu, Zhixin Yu, and Xinhai Yu. *Selection of appropriate biogas upgrading technology-a review of biogas cleaning, upgrading and utilisation.* 2015. DOI: `10.1016/j.rser.2015.06.029` (cit. on p. 16).

[35] E. Ryckebosch, M. Drouillon, and H. Vervaeren. «Techniques for transformation of biogas to biomethane». In: *Biomass and Bioenergy* 35.5 (2011), pp. 1633–1645. ISSN: 09619534. DOI: `10.1016/j.biombioe.2011.02.033`. URL: `http://dx.doi.org/10.1016/j.biombioe.2011.02.033` (cit. on p. 17).

[36] Margareta Persson, Owe Jonsson, and Arthur Wellinger. «Biogas Upgrading To Vehicle Fuel Standards and Grid». In: *IEA Bioenergy* (2007), pp. 1–32 (cit. on p. 17).

[37] Fredric Bauer, Christian Hulteberg, Tobias Persson, and Daniel Tamm. «Biogas upgrading – Review of commercial technologies». In: (2013) (cit. on p. 18).

[38] Qingrong Qian, Motoi Machida, and Hideki Tatsumoto. «Textural and surface chemical characteristics of activated carbons prepared from cattle manure compost». In: *Waste Management* 28.6 (2008). ISSN: 0956053X. DOI: `10.1016/j.wasman.2007.03.029` (cit. on p. 18).

[39] Filippo Marchelli, Eleonora Cordioli, Francesco Patuzzi, Elena Sisani, Linda Barelli, Marco Baratieri, Elisabetta Arato, and Barbara Bosio. «Experimental study on H2S adsorption on gasification char under different operative conditions». In: *Biomass and Bioenergy* 126 (2019). ISSN: 18732909. DOI: `10.1016/j.biombioe.2019.05.003` (cit. on pp. 18, 28).

[40] Prangya R. Rout, Tian C. Zhang, Puspendu Bhunia, and Rao Y. Surampalli. «Treatment technologies for emerging contaminants in wastewater treatment plants: A review». In: *Science of the Total Environment* 753 (2021). ISSN: 18791026. DOI: `10.1016/j.scitotenv.2020.141990` (cit. on p. 19).

[41] Simone Cavenati, Carlos A. Grande, and Alírio E. Rodrigues. «Separation of CH4 / CO2 / N2 mixtures by layered pressure swing adsorption for upgrade of natural gas». In: *Chemical Engineering Science* 61.12 (2006). ISSN: 00092509. DOI: `10.1016/j.ces.2006.01.023` (cit. on p. 19).

[42] Ranjani V. Siriwardane, Ming Shing Shen, and Edward P. Fisher. «Adsorption of CO2, N2, and O2 on natural zeolites». In: *Energy and Fuels* 17.3 (2003). ISSN: 08870624. DOI: `10.1021/ef020135l` (cit. on p. 19).

[43] Russamee Sitthikhankaew, David Chadwick, Suttichai Assabumrungrat, and Navadol Laosiripojana. «Effects of humidity, O2, and CO2 on H2S adsorption onto upgraded and KOH impregnated activated carbons». In: *Fuel Processing Technology* 124 (2014). ISSN: 03783820. DOI: `10.1016/j.fuproc.2014.03.010` (cit. on pp. 19, 20).

[44] J. Hofmann, K. Nachtmann, O. Falk, S. Baum, and M. Fuchsz. «Pressureless cryogenic conversion of biogas into liquefied biomethane and solid carbon dioxide». In: *European Biomass Conference and Exhibition Proceedings*. Vol. 2016. 24thEUBCE. 2016 (cit. on pp. 20, 21).

[45] Deliverable Number et al. «Unlocking unused bio-WASTE resources with loW cost cleAning and Thermal inTegration with Solid oxide fuel cells 24». In: (2019) (cit. on pp. 22, 31).

[46] *C&CS: Fuel Cell Catalysts and Adsorbents*. URL: `https://www.candcs.eu/en/processes/fuel-cell-catalysts-and-adsorbents.html` (visited on 09/29/2021) (cit. on p. 23).

[47] *C&CS: Fuel Cell Catalysts and Adsorbents.* URL: `https://www.candcs.eu/en/processes/fuel-cell-catalysts-and-adsorbents.html` (visited on 09/29/2021) (cit. on p. 23).

[48] *Arol Energy: Arol Energy |Traite et valorise le biogaz pour la production d'une énergie renouvelable présent en Savoie et intervention France entière.* URL: `http://www.arol-energy.com/accueil/` (visited on 09/29/2021) (cit. on p. 23).

[49] *Biocustom | Additivi per biogas - Miglioramento digestione e desolforazione.* URL: `https://www.biocustom.it/prodotti-tecnici-materie-prime/additivi-biogas/` (visited on 09/29/2021) (cit. on p. 23).

[50] *Biocustom | Additivi per biogas - Miglioramento digestione e desolforazione.* URL: `https://www.biocustom.it/prodotti-tecnici-materie-prime/additivi-biogas/` (visited on 09/29/2021) (cit. on p. 23).

[51] *Biocustom | Additivi per biogas - Miglioramento digestione e desolforazione.* URL: `https://www.biocustom.it/prodotti-tecnici-materie-prime/additivi-biogas/` (visited on 09/29/2021) (cit. on p. 23).

[52] *Sorbents | Desulfurization – SulfaTrap.* URL: `https://sulfatrap.com/sulfatrap-products/sorbents/` (visited on 09/29/2021) (cit. on p. 23).

[53] Adelaide S. Calbry-Muzyka, Andreas Gantenbein, Jörg Schneebeli, Alwin Frei, Amy J. Knorpp, Tilman J. Schildhauer, and Serge M.A. Biollaz. «Deep removal of sulfur and trace organic compounds from biogas to protect a catalytic methanation reactor». In: *Chemical Engineering Journal* 360 (2019). ISSN: 13858947. DOI: `10.1016/j.cej.2018.12.012` (cit. on pp. 27, 28).

[54] Christian Frilund, Pekka Simell, Noora Kaisalo, Esa Kurkela, and Mari Leena Koskinen-Soivi. «Desulfurization of Biomass Syngas Using ZnO-Based Adsorbents: Long-Term Hydrogen Sulfide Breakthrough Experiments». In: *Energy and Fuels* 5 (2020). ISSN: 15205029. DOI: `10.1021/acs.energyfuels.9b04276` (cit. on p. 28).

[55] *Final Report Summary - MCFC-CONTEX (MCFC catalyst and stack component degradation and lifetime: Fuel Gas CONTaminant effects and EXtraction strategies) | FP7 | CORDIS | European Commission.* URL: `https://cordis.europa.eu/project/id/245171/reporting/it` (visited on 10/01/2021) (cit. on p. 28).

[56] *Purification du biogaz pour sa valorisation énergétique : adsorption de siloxanes sur charbons actifs.* URL: `https://tel.archives-ouvertes.fr/tel-02887086/document` (visited on 06/05/2021) (cit. on p. 28).

[57] *Product overview: Leopold Siegrist GmbH.* URL: http://www.siegrist.de/produktuebersicht.html?tx%7B%5C_%7Dptsgproductfinder%7B%5C_%7Dpi1[category%7B%5C_%7Duid]=20%7B%5C&%7DL=1 (visited on 10/01/2021) (cit. on p. 35).